

## Rothamsted Repository Download

### A - Papers appearing in refereed journals

Prins, A., Mukubi, J. M., Pellny, T. K., Verrier, P. J., Beyene, G., Lopes, M. S., Emami, K., Treumann, A., Lelarge-Trouverie, C., Noctor, G., Kunert, K. J., Kerchev, P. and Foyer, C. H. 2011. Acclimation to high CO<sub>2</sub> in maize is related to water status and dependent on leaf rank. *Plant, Cell & Environment*. 34 (2), pp. 314-331.

The publisher's version can be accessed at:

- <https://dx.doi.org/10.1111/j.1365-3040.2010.02245.x>

The output can be accessed at: <https://repository.rothamsted.ac.uk/item/8q7q0>.

© Please contact [library@rothamsted.ac.uk](mailto:library@rothamsted.ac.uk) for copyright queries.

# Acclimation to high CO<sub>2</sub> in maize is related to water status and dependent on leaf rank

ANNEKE PRINS<sup>1</sup>, JOSEPHINE MUCHWESI MUKUBI<sup>1</sup>, TILL K. PELLNY<sup>2</sup>, PAUL J. VERRIER<sup>3</sup>, GETU BEYENE<sup>1</sup>, MARTA SILVA LOPES<sup>4</sup>, KAVEH EMAMI<sup>5</sup>, ACHIM TREUMANN<sup>5</sup>, CAROLINE LELARGE-TROUVERIE<sup>6</sup>, GRAHAM NOCTOR<sup>6</sup>, KARL J. KUNERT<sup>1</sup>, PAVEL KERCEV<sup>7</sup> & CHRISTINE H. FOYER<sup>7</sup>

<sup>1</sup>Forestry and Agricultural Biotechnology Institute, Plant Science Department, University of Pretoria, Pretoria 0002, South Africa, <sup>2</sup>Centre for Crop Genetic Improvement, Department of Plant Sciences and, <sup>3</sup>Centre for Mathematical and Computational Biology, Department of Biomathematics and Bioinformatics, Rothamsted Research, Harpenden, Hertfordshire, UK, <sup>4</sup>CIMMYT, Apdo. Postal 6-641, 06600 México, D.F., Mexico, <sup>5</sup>NEPAF Proteome Analysis Facility, Newcastle University, Newcastle upon Tyne, NE1 7RU, UK, <sup>6</sup>Institut de Biologie des Plantes, Université de Paris sud XI, 91405 Orsay cedex, France and <sup>7</sup>Centre for Plant Sciences, Institute of Integrative and Comparative Biology, Faculty of Biological Sciences, University of Leeds, Leeds, LS2 9JT, UK

## ABSTRACT

The responses of C<sub>3</sub> plants to rising atmospheric CO<sub>2</sub> levels are considered to be largely dependent on effects exerted through altered photosynthesis. In contrast, the nature of the responses of C<sub>4</sub> plants to high CO<sub>2</sub> remains controversial because of the absence of CO<sub>2</sub>-dependent effects on photosynthesis. In this study, the effects of atmospheric CO<sub>2</sub> availability on the transcriptome, proteome and metabolome profiles of two ranks of source leaves in maize (*Zea mays* L.) were studied in plants grown under ambient CO<sub>2</sub> conditions (350 ± 20 µL L<sup>-1</sup> CO<sub>2</sub>) or with CO<sub>2</sub> enrichment (700 ± 20 µL L<sup>-1</sup> CO<sub>2</sub>). Growth at high CO<sub>2</sub> had no effect on photosynthesis, photorespiration, leaf C/N ratios or anthocyanin contents. However, leaf transpiration rates, carbohydrate metabolism and protein carbonyl accumulation were altered at high CO<sub>2</sub> in a leaf-rank specific manner. Although no significant CO<sub>2</sub>-dependent changes in the leaf transcriptome were observed, qPCR analysis revealed that the abundance of transcripts encoding a Bowman–Birk protease inhibitor and a serpin were changed by the growth CO<sub>2</sub> level in a leaf rank specific manner. Moreover, CO<sub>2</sub>-dependent changes in the leaf proteome were most evident in the oldest source leaves. Small changes in water status may be responsible for the observed responses to high CO<sub>2</sub>, particularly in the older leaf ranks.

**Key-words:** CO<sub>2</sub> assimilation; CO<sub>2</sub> enrichment; protease inhibitors; redox regulation; sugar signalling.

## INTRODUCTION

Global atmospheric CO<sub>2</sub> concentrations have risen from about 270 µL L<sup>-1</sup> in pre-industrial times to the present level of over 380 µL L<sup>-1</sup>. Values are predicted to reach between 530 and 970 µL L<sup>-1</sup> by the end of this century. Moreover, the

capacity of the earth's oceans to absorb CO<sub>2</sub> from the atmosphere is considered to be reaching saturation point (Khatiwala, Primeau & Hall 2009). Average global temperatures have increased by about 0.76 °C over the last 150 years and they are likely to increase by another 1.7 to 3.9 °C during this century. In theory, plants could mitigate these changes through photosynthetic conversion of atmospheric CO<sub>2</sub> into carbohydrates and other organic compounds. However, the potential for this mitigation remains uncertain and the impact of predicted increases in atmospheric CO<sub>2</sub> and global temperatures on plant productivity is a growing concern for agriculture and food security worldwide (Long *et al.* 2004; Long *et al.* 2006). In plants that use the C<sub>3</sub> pathway of photosynthesis, the predicted changes in atmospheric CO<sub>2</sub> concentrations and the temperature of the earth will directly influence the balance between photosynthetic carbon fixation and photorespiration, and also plant C/N relationships as atmospheric CO<sub>2</sub> enrichment inhibits the assimilation of nitrate into organic nitrogen compounds (Foyer *et al.* 2009). The anticipated changes in the Earth's environment will therefore influence partitioning between these pathways, and as a consequence influence the distribution of plants with different carbon fixation pathways (Ward *et al.* 1999; Ward *et al.* 1999; Zhu, Goldstein & Bartholomew 1999). In the C<sub>3</sub> pathway of photosynthesis, CO<sub>2</sub> enters the Benson-Calvin cycle directly by the action of ribulose 1, 5-bisphosphate carboxylase oxygenase (Rubisco). In contrast, the C<sub>4</sub> pathway of photosynthesis incorporates an endogenous CO<sub>2</sub>-concentrating mechanism where CO<sub>2</sub> is first incorporated into organic acids in the mesophyll cells. By virtue of this CO<sub>2</sub>-concentrating mechanism CO<sub>2</sub>-limitations at the Rubisco active site in the bundle sheath cells are diminished. Hence, increasing atmospheric CO<sub>2</sub> is predicted to have less impact on plants with the C<sub>4</sub> pathway of photosynthesis than their C<sub>3</sub> counterparts.

Elevated CO<sub>2</sub> concentrations decrease photorespiration and initially enhance photosynthesis and growth as much as 35% in most C<sub>3</sub> plants (Long *et al.* 2004; Long *et al.* 2006).

Correspondence: C. H. Foyer. e-mail: c.foyer@leeds.ac.uk

The high CO<sub>2</sub>-dependent enhancement of photosynthesis, however, diminishes over time (days to years), a phenomenon known as CO<sub>2</sub> acclimation (Paul & Foyer 2001). This process, which involves loss of Rubisco protein and activity, is largely absent from C<sub>4</sub> plants, where these enzymes have already acclimated to functioning under high CO<sub>2</sub> conditions. However, there is considerable variation in the responses of different C<sub>4</sub> species to enhanced CO<sub>2</sub> (Maroco, Edwards & Ku 1999; Ward *et al.* 1999; Ziska & Bunce 1999; Cousins *et al.* 2001). Some C<sub>4</sub> plants show acclimation to high CO<sub>2</sub> (Soares *et al.* 2007) this is generally not related to effects on photosynthesis, which is largely unchanged (Sage 1994; Ghannoum *et al.* 1997, 2001; Wand, Midgley & Stock 2001; Leakey *et al.* 2006).

Atmospheric CO<sub>2</sub> availability exerts a strong influence on stomatal density and patterning (Taylor *et al.* 1994, 2008; Larkin *et al.* 1997; Croxdale 1998; Masle 2000; Lake *et al.* 2001; Lake, Woodward & Quick 2002; Poorter & Navas 2003; Martin & Glover 2007). Signals concerning CO<sub>2</sub> availability appear to be transmitted from older to developing leaves in C<sub>3</sub> plants (Lake *et al.* 2001, 2002; Woodward 2002). Growth at enhanced atmospheric CO<sub>2</sub> concentrations often leads to a decrease in stomatal density (Woodward, Lake & Quick 2002). However, this acclimation response varies considerably between species (Woodward & Kelly 1995). High CO<sub>2</sub>-dependent increases in stomatal index have been observed in two monocotyledonous C<sub>4</sub> species, maize and *Paspalum dilatatum* (Driscoll *et al.* 2006; Soares *et al.* 2007; Soares-Cordeiro *et al.* 2009). The CO<sub>2</sub>-signalling pathways that orchestrate such changes in epidermal patterning and leaf structure, function and composition remain poorly characterized (Gray *et al.* 2000; Ferris *et al.* 2002), but it is generally accepted that the signals that regulate such responses are systemic in nature (Coupe *et al.* 2006; Miyazawa, Livingston & Turpin 2006). Carbonic anhydrases have recently been considered to be important components of plant CO<sub>2</sub>-signalling pathways (Hu *et al.* 2010). *Arabidopsis thaliana* double-mutants lacking two B-carbonic anhydrases (B-CA1 and B-CA4) higher stomatal densities but impaired stomatal movements in response to changing CO<sub>2</sub> levels (Hu *et al.* 2010).

The stability of internal CO<sub>2</sub> (C<sub>i</sub>) with changing CO<sub>2</sub> fixation rates suggests that leaves are able to sense and signal information concerning C<sub>i</sub> (Warren 2008), rather than atmospheric CO<sub>2</sub> (Mott 1988). The guard cells of stomata are able to sense an array of endogenous and environmental signals including CO<sub>2</sub> availability. Atmospheric CO<sub>2</sub> can induce either stomatal opening or closure depending on concentration by influencing the patterns of repetitive calcium transients within the guard cells that are linked to changes in ion channel activities and potassium efflux. Like abscisic acid (ABA), high CO<sub>2</sub> participates in a complex network of signalling events that cause an inhibition of K<sup>+</sup> inward rectifying channels and an activation of K<sup>+</sup> outward rectifying channels that enhances potassium efflux and consequently results in stomatal closure (Acharya & Assmann 2009).

The regulation of stomatal closure in relation to C<sub>i</sub> is complex (von Caemmerer *et al.* 2004; Baroli *et al.* 2008; Mott, Sibbersen & Shope 2008), and probably involves signals in the vapor phase that transmit information concerning the redox state of the chloroplast. However, compared with the extensive literature on systemic light signalling responses (Karpinski *et al.* 1999; Rossel *et al.* 2007; Muhlenbock *et al.* 2008), little information is available concerning systemic CO<sub>2</sub> signalling pathways in plants (Baroli *et al.* 2008; Mott *et al.* 2008) and very few CO<sub>2</sub> signalling components have been identified (Gray *et al.* 2000). Systemic light signalling is triggered by the photosynthetic electron transport chain in the high-light-exposed leaves and involves salicylic acid (SA)-, jasmonic acid (JA)- and ethylene (ET)-dependent pathways (Karpinski *et al.* 1999; Fryer *et al.* 2003; Rossel *et al.* 2007; Muhlenbock *et al.* 2008). Here, we have studied how the leaves of maize, an economically important C<sub>4</sub> species, respond to enhanced atmospheric CO<sub>2</sub> availability. Maize plants were grown for up to 8 weeks either under the ambient CO<sub>2</sub> conditions of our laboratories (350 ± 20 μL L<sup>-1</sup> CO<sub>2</sub>) or with CO<sub>2</sub> enrichment (700 ± 20 μL L<sup>-1</sup> CO<sub>2</sub>). We have combined classic whole plant physiology and -omics approaches to characterize the acclimation of two ranks of maize source leaves to high CO<sub>2</sub> and to use this information to provide information on possible CO<sub>2</sub> signalling mechanisms.

## MATERIALS AND METHODS

### Plant material and growth conditions

*Zea mays* L. hybrid H99 plants were grown for up to 8 weeks in compost (Driscoll *et al.* 2006) in duplicate controlled environment cabinets (Sanyo 970, Sanyo, Osaka, Japan) where the atmospheric CO<sub>2</sub> was maintained at either 350 μL L<sup>-1</sup> or at 700 μL L<sup>-1</sup>. In total six controlled environment cabinets were used in these experiments. Each cabinet contained plants grown under one of the conditions earlier, i.e. either 'ambient' conditions or 'high CO<sub>2</sub>'. In total, three cabinets were set at the ambient CO<sub>2</sub> levels whereas the other three were maintained at the high CO<sub>2</sub> level. The data or harvests obtained from plants in each cabinet were pooled so that there is a one-to-one match of cabinets and pools.

In all cases, the plants were grown with a 16 h photoperiod (700 μmol m<sup>-2</sup> s<sup>-1</sup>) and the temperature was maintained at 25 °C (day) and 19 °C (night) with 80% relative humidity. The CO<sub>2</sub> was supplied from a bulk container, transmitted via a Vaisala GMT220 CO<sub>2</sub> transmitter (Vaisala Oyj, Helsinki, Finland), and maintained by a Eurotherm 2704 controller (Eurotherm Ltd., Worthing, UK), which kept CO<sub>2</sub> levels at 350 ± 20 μL L<sup>-1</sup> or 700 ± 20 μL L<sup>-1</sup>. All plants were watered daily throughout development in order to avoid a water stress. Leaf samples were harvested 11 h into the photoperiod from plants at 3 (six leaves), 6 (nine leaves) and 8 (13 leaves) weeks of growth.

### Leaf parameters, water use efficiencies and photosynthesis measurements

The whole leaf weight and leaf area measurements were performed on each leaf rank at the 13-leaf stage. Leaf area measurements were performed using a  $\Delta T$  area meter (Delta-T Devices Ltd., Cambridge, England). Intrinsic water use efficiencies were determined according to Soares-Cordeiro *et al.* (2009). Photosynthetic gas exchange measurements were performed as described previously (Driscoll *et al.* 2006).

### Anthocyanin, chlorophyll and pheophytin determinations

Fresh weight and dry weight measurements were performed on each leaf rank at the 13-leaf stage. Leaf discs (8 cm<sup>2</sup>) were cut from the centre of each leaf. Leaf mass was measured before and after the tissue was dried in an oven for 3 d at 60°C. Leaf anthocyanins were extracted and assayed in separate maize discs harvested as earlier, according to Sims & Gamon (2002). Chlorophyll was measured in the same tissues according to Wintermans & De Mots (1965) and the pheophytin content was determined according to Vernon (1960).

### Metabolome and amino acid analyses

Samples from leaf rank 5 on 9-week-old plants were harvested and frozen immediately in liquid nitrogen. Four independent extracts per plant were analyzed by gas chromatography time-of-flight mass spectrometry (GC-TOF MS), using a method adapted from Noctor *et al.* (2007). Ninety-four derivatives corresponding to 88 unique metabolites were identified by reference to their mass spectra. Peak intensities were normalized to an internal standard (ribitol) and then to leaf chlorophyll contents, and metabolites showing a statistically significant difference between the two conditions were identified by *t*-test ( $P < 0.05$ ).

### Leaf temperature and total C and N contents

Leaf temperature was measured on all leaf ranks of 3-week-old plants. Whole leaves were then harvested and frozen immediately in liquid nitrogen. Total C and N contents were measured by elemental analysis (EA1108, Series 1, Carlo Erba Istrumentazione, Milan, Italy).

### Measurements of leaf sucrose, hexoses and starch

Leaf sucrose, hexoses and starch measurements were performed on each leaf rank at 13-leaf stage. Whole leaves were harvested and immediately frozen in liquid nitrogen in the growth cabinets. Leaf sucrose and hexose were extracted and assayed according to Jones, Outlaw & Lowry

(1977). Starch was extracted and assayed in the same samples according to the method of Paul & Stitt (1993).

### Measurement of the extent of leaf protein carbonylation

Protein carbonylation assays were performed on each leaf rank at 13-leaf stage. Whole leaves were harvested and immediately frozen in liquid nitrogen in the growth cabinets. The composition and extent of protein carbonyl group formation was measured using the OxyBlot™ Oxidized Protein Detection Kit (Chemicon International, Harrow, UK).

### RNA extraction methods

Micro-analyses were performed on samples (in triplicate) of rank 3 and rank 12 leaves from separate plants at 13-leaf stage. Three separate sets of leaf samples were prepared per leaf rank and per treatment. Each individual sample was made up of three whole pooled leaves taken from three separate plants. The samples were as follows: (1) leaf rank 3 under ambient CO<sub>2</sub> conditions; (2) leaf rank 12 under ambient CO<sub>2</sub> conditions; (3) leaf rank 3 under high CO<sub>2</sub> conditions; and (4) leaf rank 12 under high CO<sub>2</sub> conditions. Total RNA was extracted using Trizol reagent (Invitrogen, Paisley, UK).

For qPCR, RNA was extracted from pooled samples of three biological replicates grown in either air or with CO<sub>2</sub> enrichment, representing each leaf on the stem. For the feeding study, total RNA was extracted from 400 mg of frozen tissue obtained from pooled tissue of 10 biological replicates. Total RNA was purified with RNeasy Mini Spin Columns (Qiagen GmbH, Hilden, Germany).

### Microarray hybridization techniques

Purified RNA samples were sent to ArosAB, Aarhus, Denmark, where they were converted to cDNA and used to synthesize biotin-labelled cRNA (BioArray High Yield RNA Transcript Labeling Kit, Enzo, Farmingdale, NY, USA). Labelled cRNA was hybridized to maize microarray chips (Affymetrix, Santa Clara, CA, USA) for samples isolated from air-grown plants giving rise to 12 microarray chips representing three biological replicates of the young and old plants grown in air and high CO<sub>2</sub> levels. The corn microarrays cover approximately 14 k probesets, which represent less than 10 k genes. Each chip was washed and scanned in a GeneChip Scanner 3000 (Affymetrix). Microarray data are available in the ArrayExpress database (<http://www.ebi.ac.uk/arrayexpress>) under accession number E-MEXP-1222.

### Microarray analysis

Gene expression profiles were then compared using GeneSpring GX 11.00. The *P*-values were calculated by

asymptotic unpaired *t*-test and subjected to multiple testing correction (Benjamini Hochberg FDR). A cut-off with *P*-value < 0.05 and log<sub>2</sub> expression ratio ± 1 was adopted. The probe targets were as defined by Affymetrix (<https://www.affymetrix.com/analysis/netaffx/index.affx>) and these targets were used to guide annotation of the genes through the use of BLAST against the TAIR (<http://www.arabidopsis.org/>) database. Transcripts were identified according to Unigene cluster (<http://www.ncbi.nlm.nih.gov/UniGene>; Pontius, Wagner & Schuler 2003) and translated homology search (tblastx) on the NCBI protein refseq database and on the trembl (EBI) data set with the criteria of minimum score of 50% and *e*-value of ≤10<sup>-7</sup> for selecting potentially significant homology to the Affymetrix supplied target sequences as the subjects for comparison.

### Sugar and pro-oxidant treatments

Ten leaves from plants grown in ambient CO<sub>2</sub> were cut into sections (1 cm<sup>2</sup>) under 10 mM Hepes buffer (pH 7.0). The leaf sections (30 per treatment) were incubated in 10 mM Hepes buffer (pH 7.0) alone or buffer containing 50 mM fructose, 50 mM glucose, 50 mM sucrose, 20 mM H<sub>2</sub>O<sub>2</sub> or 1 mM methyl viologen. Leaf sections were incubated for 16 h in the dark in the above solutions, after which time the leaf sections were harvested for real-time (qPCR) analysis.

### Real-time (qPCR) analysis

Purified total RNA was first treated with DNase I (amplification grade; Invitrogen). The first strand cDNA was then prepared using SuperScript II (Invitrogen). Quantitative PCR was performed using this template. Sequences for ubiquitin, thioredoxin and cyclophilin were selected as endogenous controls based on their equal expression values on microarray analysis. Primers were designed to amplify 50–53 bp amplicons present in the probesets on the microarray chips. Quantitative PCR was performed at least in triplicate using the Applied Biosystems 7500 Real-time PCR System (Applied Biosystems, Cheshire, UK) and SYBR green as intercalating dye (Sigma, Dorset, UK) with the following cycling profile: 1 × 50 °C (2 min), 1 × 95 °C (10 min), 40 × [95 °C (15 s), 60 °C (1 min)]. Relative quantitative analysis of transcripts was performed using the Applied Biosystems Detection Software (SDS) v1.2.1. Relative expression values were confirmed in each case by at least two endogenous controls.

### Isolation of full-length serine-type protease inhibitors

Total RNA was extracted from leaf three pooled samples from six maize seedlings at the five-leaf stage using the TriPure total RNA isolation kit with contaminant genomic DNA digested by RNase-free DNase. Total RNA (2 µg per sample) that had been subjected to reverse transcription using superscript III<sup>TM</sup> Reverse Transcriptase (RT) (Invitrogen, Carlsbad, CA, USA) was used as a template

in the PCR reaction. Full-length cDNA clones for the *Zea mays* serine-type endopeptidase inhibitor (accession numbers EF406275) and Bowman–Birk-type serine protease inhibitor (accession number EF406276) were obtained by performing 5′ and 3′ rapid amplification of cDNA ends (RACE) using the GeneRacer<sup>TM</sup> kit (Invitrogen) together with gene-specific primers. Gene-specific primers (forward 5′-tactcagctcaaggtgaaggcagtg-3′ and reverse 5′-cgaatcagcactcttggttcagag-3′) were used for isolation of a full-length serine-type endopeptidase inhibitor and primers (forward 5′-cctcagctgatactcgtcgact-3′ and reverse 5′-gaactcgtcagcagcgtaggtga-3′) were used for isolation of a full-length Bowman–Birk-type serine proteinase inhibitor. The 5′ RACE, 5′ nested, 3′ RACE and 3′ nested primers were provided with the GeneRacer<sup>TM</sup> kit (Invitrogen) that were used together with the gene specific primers. All amplified PCR products were T/A cloned into PCR4-TOPO (which was also provided with GeneRacer Kit) and sequenced in both direction using M13 forward and reverse primers. Inserts were sequenced using the BigDye<sup>®</sup> Terminator Cycle Sequencing FS Ready Reaction Kit, v 3.1 on ABI PRISM<sup>®</sup> 3100 automatic DNA-Sequencer (Applied Biosystems, Foster City, CA, USA). The BLASTn and BLASTp programs (Altschul *et al.* 1990) were used for gene sequence homology search.

### Analysis of putative serpin and BBI sequence isolated from maize

The cDNA sequences of EF406275 (putative serpin) and EF406276 (putative BBI) were analysed using online tools: BLASTx at GenBank (Altschul *et al.* 1990), WU-blastn V2.0 (<http://blast.wustl.edu/>; Gish & States 1993) on the EMBL database, ORF finder (<http://www.ncbi.nlm.nih.gov/gorf/gorf.html>), ProtParam and TargetP (<http://www.cbs.dtu.dk/services/TargetP/>; Emanuelsson *et al.* 2000).

### Phylogenetic analysis of putative serpin and BBI sequences

After identification of their coding sequences, protein homologs of the putative serpin and putative BBI genes were identified by translated homology search (BLASTx) at GenBank. Translated gene sequences were compared with protein homologs by phylogenetic comparison, the alignments being determined by ClustalW (as implemented in the VectorNTI package), and the best unrooted tree was generated with PAUP4\* in default parameter configuration and the resultant trees were displayed using the PhyloDraw package. Sequence data from this article can be found in the EMBL/GenBank data libraries under accession number EF406275 and EF406276

### Proteomic analysis

Leaf extracts prepared from leaf 3 and leaf 12 of 8-week-old plants were prepared for two-dimensional (2D)

electrophoresis according to instructions in the handbook *2-D Electrophoresis: Principles and Methods* (GE Healthcare, Piscataway, NJ, USA). Three technical replicates were prepared from each extraction. Proteins were precipitated after grinding leaf material in liquid nitrogen. Ground leaf material (200–250 mg) was incubated overnight at  $-20^{\circ}\text{C}$  in precipitation buffer (1 mL) containing TCA (10%, w/v) and  $\beta$ -mercaptoethanol (0.07% v/v) in acetone (100%, v/v). Precipitated protein was pelleted by centrifuging for 25 min at  $4^{\circ}\text{C}$  at 20 000 g and washed six times with ice cold washing buffer containing acetone (90%, v/v) and  $\beta$ -mercaptoethanol (0.07% v/v) in Milli-Q water. Proteins were solubilized in sample buffer (1 mL) containing urea (8 M), CHAPS (2%, w/v), dithiothreitol (DTT; 60 mM), and IPG buffer pH 4–7 (0.5%, v/v) (GE Healthcare), by sonication in an ultrasonic water bath for 1 h, with vortexing at 15 min intervals. Samples were then incubated in a heating block for 1.5 h at  $30^{\circ}\text{C}$  with vortexing at 15 min intervals before overnight incubation at room temperature for optimal protein solubilization. Cell debris was removed by centrifugation for 25 min at 20 000 g. Solubilized proteins were quantified using the Bradford assay (Bradford 1976) and ovalbumin (Sigma) as standard (Ramagli 1999). Four hundred fifty micrograms of the protein extracts were diluted in 250  $\mu\text{L}$  rehydration buffer (7 M urea, 2 M thio-urea, 0.75% (w/v) CHAPS, 0.75% (v/v) Triton X 100, 100 mM DTT, a trace of bromophenol blue, 2% (v/v) IPG buffer pH 4–7; GE Healthcare). Samples were then loaded onto 13 cm immobilized DryStrip gels pH 4–7 (GE Healthcare) and run on an Ettan IPGphor II (GE Healthcare; rehydration, 20 h at  $20^{\circ}\text{C}$ ; 500 V for 1 h; 500 to 1000 V in 1 h; 1000 to 8000 V in 2:30 h; and hold at 8000 V for 55 min). IPG strips were then equilibrated first for 20 min in 50 mM Tris-HCl (pH 8.8), 6 M urea, 30% (w/v) glycerol, 2.3% (w/v) SDS, 1% (w/v) DTT, followed by 20 min in the same solution with DTT replaced with 4% (w/v) iodoacetamide. The IPG strips were then applied to 12.5% resolving gels and were run in an SE 600 Ruby<sup>TM</sup>, gel unit (GE Healthcare) at 25 mA  $\text{gel}^{-1}$  for 5 h at  $10^{\circ}\text{C}$ . The running buffer was 25 mM Trisbase, 192 mM glycine, 0.1% SDS. Finally the gels were stained in a 0.1% solution of Phastgel-blue R-350 (GE Healthcare) in 40% methanol and 7% acetic acid overnight and destained in 40% methanol, 7% acetic acid, at room temperature on an orbital shaker. The stained gels were scanned on a calibrated Ettan Gel Imager (GE Healthcare) before being subjected to image analysis.

### Image analysis

Progenesis SameSpots software (Nonlinear Dynamics, Durham, NC, USA) was used for gel analysis. The spots were matched between all the gels by using the SameSpots approach. Background subtraction and volume normalization were carried out. Artefacts and non-protein spots were removed by editing the template image and were expanded to all gels using the SameSpots option. The gels were also subjected to detailed Progenesis statistical analysis (*t*-test). Protein spots of interest were excised using Harris spot

cutters (Sigma) before being subjected to in-gel digestion with trypsin and nano-liquid chromatography mass spectrometry (LC MS)/MS analysis.

### In-gel trypsin digest

Excised spots were washed with 25% (v/v) methanol and 7% (v/v) acetic acid for 12 h at room temperature, and de-stained with 50 mM  $\text{NH}_4\text{HCO}_3$  in 50% (v/v) methanol for 1 h at  $40^{\circ}\text{C}$ . The gel pieces were then incubated in 10 mM DTT, 100 mM  $\text{NH}_4\text{HCO}_3$  for 1 h at  $60^{\circ}\text{C}$  followed by 40 mM iodoacetamide, 100 mM  $\text{NH}_4\text{HCO}_3$  for 30 min at room temperature. The gel pieces were minced, dried, rehydrated in 100 mM  $\text{NH}_4\text{HCO}_3$  containing 1 pmol of trypsin (Promega, Madison, WI, USA) and incubated at  $37^{\circ}\text{C}$  overnight. The digested peptides were extracted from the gel slices with 0.1% TFA in 50% (v/v) acetonitrile/water three times. The peptide solution was dried, re-suspended in 30  $\mu\text{L}$  of 0.1% TFA/5% acetonitrile/water.

### LC-MS/MS

LC-MS/MS analysis was performed at NEPAF, Cels Ltd., Newcastle, UK. Using an Ultimate 3000 nano-HPLC system (Dionex LC Packings, Camberley, UK), 10% of the digest was injected at 20  $\mu\text{L}/\text{min}$  onto a 300  $\mu\text{m} \times 50$  mm PepMap trap column (Dionex). After washing with 60  $\mu\text{L}$  of 0.1% formic acid at 20  $\mu\text{L}/\text{min}$ , peptides were eluted through a 150  $\text{mm} \times 75$   $\mu\text{m}$  PepMap column (Dionex) at 200 nL/min. MS spectra were acquired on an HCT Proteome Discovery system (Bruker Daltonics, Bremen, Germany). A survey scan was conducted in standard enhanced mode (8100 Da/s) from  $m/z$  400 to  $m/z$  1600. The three most intense ions were fragmented and MS/MS scans were acquired in ultrascan mode (26 000 Da/s) from 50 to 2100 Da. Parent ions were dynamically excluded for 90 s after two MS/MS acquisitions. Up to 300 000 ions were accumulated in the linear trap with a maximum accumulation time of 120 s. Up to 750 spectra per LC/MS experiment were extracted from the data using Bruker DataAnalysis 3.4 software. MS/MS spectra were de-convoluted, converted to line spectra and exported as mgf files for homology searches. The translated *Oryza sativa* genome (as on 1 September 2008), the translated *Arabidopsis thaliana* genome (as on 1 September 2008) and a collection of frequently occurring contaminating proteins [common Repository of Adventitious Proteins (cRAP)] and their reverse counterparts were searched using X!Tandem allowing for single amino acid substitutions and the gpm web interface at <http://www.thegpm.org> (Craig & Beavis, 2004). Search parameters and results were submitted to the gpm database and can be accessed through the hyperlinked Identifier codes in the Supporting Information.

### Statistical analysis

The statistical analysis of the micro-array data is described earlier. The gas exchange data was analyzed by analysis of

variance (ANOVA). Data for all other physiological parameters was analyzed by the Student's *t*-test or least significant difference (LSD) test.

### Accession numbers

Putative serine proteinase inhibitor sequence was submitted to GenBank (<http://www.ncbi.nlm.nih.org>) with accession number EF406275. Putative Bowman-Birk inhibitor sequence was submitted to GenBanks with accession number EF406276. Microarray data are available in the ArrayExpress database (<http://www.ebi.ac.uk/arrayexpress>) under accession number E-MEXP-1222.

## RESULTS

### High CO<sub>2</sub> effects on whole plant morphology and photosynthesis

Maize plants were grown for up to 8 weeks (Fig. 1a) in either ambient CO<sub>2</sub> conditions (350 ± 20 μL L<sup>-1</sup> CO<sub>2</sub>) or with CO<sub>2</sub> enrichment (700 ± 20 μL L<sup>-1</sup> CO<sub>2</sub>). The plants grown with CO<sub>2</sub> enrichment exhibited a similar overall morphology to those grown under ambient CO<sub>2</sub> conditions (Fig. 1a). In an earlier study we reported that the maize plants grown with CO<sub>2</sub> enrichment were taller than those grown in air although they had the same number of leaves (Driscoll *et al.* 2006). However, the more systematic analysis reported here revealed that there were small variations in the specifications of the controlled environment growth chambers used previously and that these had led to differences in overall plant height (Driscoll *et al.* 2006). These small but important variations were eliminated in the present study by randomization of chamber usage. The data presented here shows that growth with CO<sub>2</sub> enrichment has no effect on the height of the maize plants.

There were no significant differences in the fresh weights (Fig. 1b), the dry weights (Fig. 1c), or tissue water contents (Fig. 1d) of leaves at equivalent positions on the stem. The leaf fresh weight values were similar regardless of ontogeny, but the dry weight values were greatest in the young leaves and decreased with leaf position on the stem (1 to 12). The leaves in ranks 1–5 had the lowest dry weight values (Fig. 1c). Similarly, the tissue water content was greatest in leaf ranks 1–5 and decreased gradually with the leaf position on the stem, the young leaves having the lowest tissue water contents (Fig. 1d). Specific leaf weight and specific leaf area values were similar under both ambient and high CO<sub>2</sub> conditions in all except the youngest leaves (Fig. 1e, f). Leaf total anthocyanin contents were highest in leaf ranks 1–4, but values were similar in plants grown in ambient conditions or with CO<sub>2</sub> enrichment (Fig. 1g).

Transpiration rates were similar at leaf rank 12 under both CO<sub>2</sub> conditions but they were decreased in the rank 5 leaves at high CO<sub>2</sub> (Fig. 2a). Stomatal conductance rates were higher at rank 12 than rank 5, the difference being most marked in plants grown at high CO<sub>2</sub> (Fig. 2b). Stomatal conductance was significantly higher at both leaf

ranks under ambient CO<sub>2</sub> conditions compared with high CO<sub>2</sub> (Fig. 2b). In line with the lower stomatal conductance rates at high CO<sub>2</sub>, leaf temperatures were higher (Table 1).

The leaves at rank 12 had significantly higher (about 30%) rates of photosynthesis than those at leaf rank 5 under both CO<sub>2</sub> conditions (Fig. 2c). However, photosynthesis rates were high at both leaf ranks and thus leaves at both ranks are denoted as 'source leaves'. Although photosynthesis rates appeared to be lower at high CO<sub>2</sub> as observed previously (Driscoll *et al.* 2006), the differences between the two CO<sub>2</sub> conditions were not significant (Fig. 2c). Photosynthesis rates were not significantly changed by the growth CO<sub>2</sub> environment (Fig. 2c). Water use efficiency values were higher in leaves at rank 12 than rank 5 under ambient CO<sub>2</sub> conditions (Fig. 2d). Growth with CO<sub>2</sub> enrichment significantly enhanced the water use efficiencies at both leaf ranks (Fig. 2d). There were no significant differences in total C or total N contents or C/N ratios in leaves grown under ambient or high CO<sub>2</sub> conditions (Table 1).

### The maize leaf transcriptome

The transcript profiles of leaf ranks 12 and 3 from plants grown under ambient and high CO<sub>2</sub> conditions were analysed. In each case, three plants were used for each RNA extraction pool (in line with the sample source being designated as 2–3 plants per sample per chip in microarray submission: E-MEXP-1222). The transcriptome profiles were similar under ambient and high CO<sub>2</sub> conditions and there were no significantly changed transcripts. In contrast, there were significant differences in transcriptomes of leaf ranks 3 and 12. This analysis revealed significant differences in 734 transcripts under ambient CO<sub>2</sub> conditions (Supporting Information Table S1) and significant differences in 738 transcripts in plants grown under conditions of CO<sub>2</sub> enrichment (Supporting Information Table S2). Of these transcripts that were specifically changed by leaf ontogeny irrespective of the CO<sub>2</sub> enrichment, 569 transcripts were the same under both CO<sub>2</sub> treatments (Fig. 3a). Leaf rank-dependent changes were observed in transcripts encoding proteins involved in nitrogen metabolism such as nitrate reductase, nitrate reductase and glutamine synthetase, which were higher in leaf rank 12 than 3. While mRNAs encoding sucrose phosphate synthetase (SPS), phosphoenol pyruvate carboxylase and β amylase (Supporting Information Table S3) were higher in leaf rank 12 than 3, transcripts encoding sucrose synthase and UDPglucose dehydrogenase were lower in leaf rank 3 than 12 (Supporting Information Table S3). Transcripts encoding metacaspases, metalloproteinases, serine proteases and cysteine proteases and cysteine protease inhibitors were also higher in leaf rank 12 than 3 (Supporting Information Table S3). We also identified a putative serine protease inhibitor and a putative BBI serine protease inhibitor that were altered in a leaf rank-specific manner (Supporting Information Table S3). The full-length gene sequences of these inhibitors were obtained by RACE and compared with those of known similar inhibitors in the

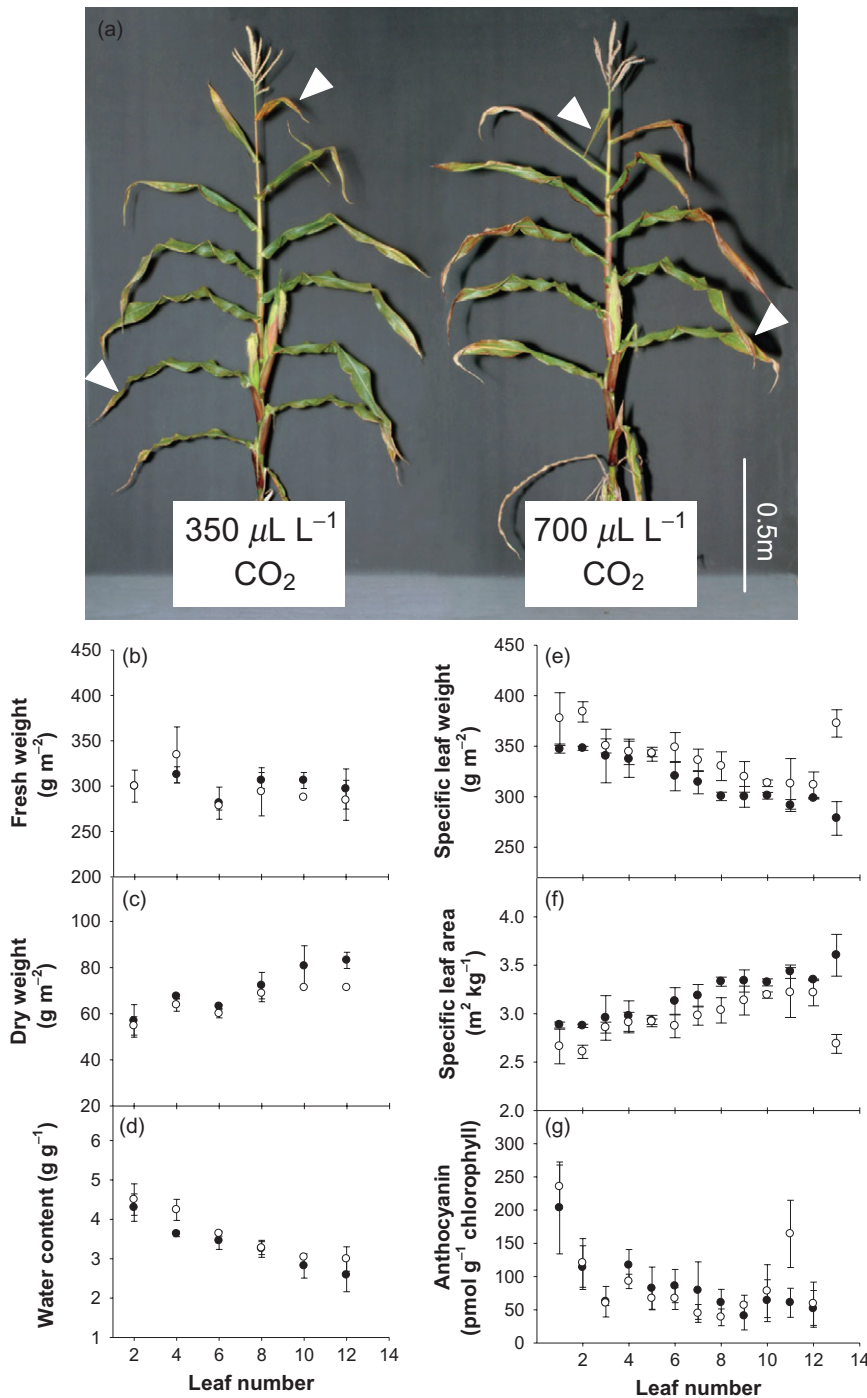


**Figure 1.** A comparison of the morphologies of 8-week-old maize plants grown under either ambient CO<sub>2</sub> conditions (350 μL L<sup>-1</sup>) or with CO<sub>2</sub> enrichment (700 μL L<sup>-1</sup>). Whole plant phenotype (a) showing the ranking of all leaves on the stem. Samples were harvested from plants grown under either ambient CO<sub>2</sub> conditions (closed circles) or with CO<sub>2</sub> enrichment (open circles). Fresh weight (b) and dry weight (c) values were used to calculate tissue water content (d). Specific leaf weight (e). Specific leaf area (f). Leaf anthocyanin content (g). Significant differences at  $P < 0.05$  indicated by the symbol (\*).

databases (Figs 3b, c & 4 Table 4). The putative serine protease inhibitor EF406275 (serpin) was identified through homology to an *Arabidopsis* serine-type endopeptidase inhibitor (NP\_177351.1; bit score 86.3;  $E = 6e-16$ ). The BBI sequence has a high sequence similarity to a patented maize

sequence, which is described as a maize proteinase inhibitor-like polynucleotide (AR494954; patent number US6720480-A/1, 13-APR-2004).

Although no significant effects of atmospheric growth CO<sub>2</sub> on the leaf transcript profile were found in the

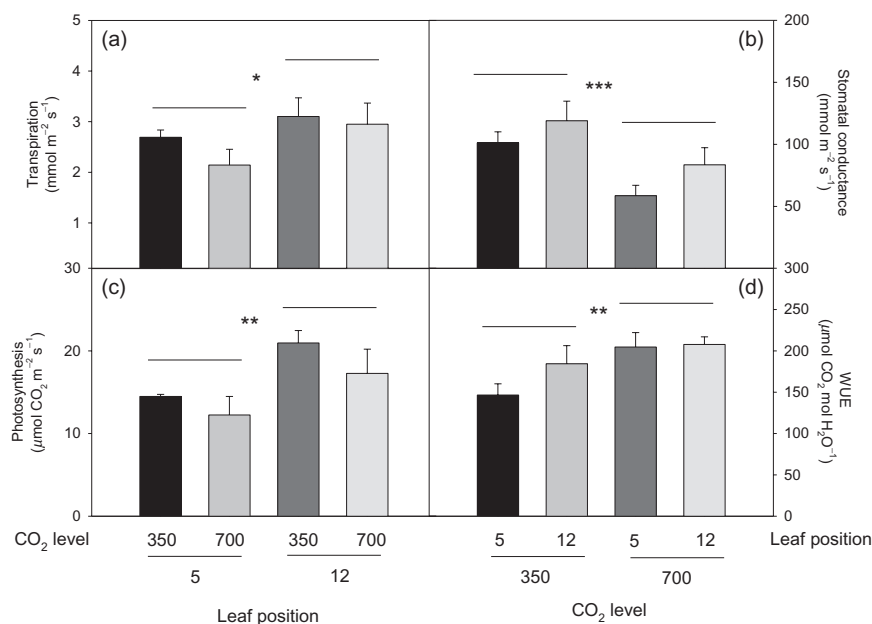


**Figure 2.** Comparison of transpiration rates (a), stomatal conductance (b) photosynthesis (c) and water use efficiencies (WUE, D) in source leaves at ranks 5 and 12 on plants that had been grown for 8 weeks under either ambient CO<sub>2</sub> conditions (350 ± 20 μL L<sup>-1</sup>) or with CO<sub>2</sub> enrichment (700 ± 20 μL L<sup>-1</sup>). Values represent mean ± SE; *n* = 4. Data were analysed by two-factorial analysis of variance and significant differences between treatments are displayed (\* at 10%, \*\* at 5%, \*\*\* at 1%).

transcriptome analysis, the effects of growth CO<sub>2</sub> on the abundance of certain transcripts were also examined using qPCR. For this analysis we compared the transcripts encoding the two serine protease inhibitors and four invertase and sucrose synthase sequences associated with carbohydrate metabolism (cell wall invertase, acid invertase, two sucrose synthase forms, and sucrose phosphate synthase) in leaves of plants grown either under ambient CO<sub>2</sub> conditions or with CO<sub>2</sub> enrichment. Under ambient CO<sub>2</sub> conditions the abundance of the serpin transcripts was dependent on leaf rank, with the highest levels in leaf ranks 1–3 (Fig. 5a). The abundance of the BBI transcripts was also dependent on the position of the leaf on the stem (Fig. 5a, b). While serpin transcripts were increased as a result of growth with CO<sub>2</sub> enrichment in the youngest source leaves (Fig. 5a), BBI transcripts showed a CO<sub>2</sub>-dependent change in abundance only in the oldest source leaves (Fig. 5b). Although growth with CO<sub>2</sub> enrichment had no effect on the abundance of cell wall invertase, sucrose synthase and sucrose phosphate synthase transcripts (Fig. 5c–g), the abundance of acid invertase was higher in leaves of plants grown at high CO<sub>2</sub> (Fig. 5c). The abundance of SPS transcripts was dependent

on leaf rank with the highest levels measured in the youngest source leaves (Fig. 5g). Less marked effects of leaf rank were found for transcripts encoding cell wall invertase, acid invertase, and the two sucrose synthase forms.

### CO<sub>2</sub>-dependent effects on the leaf proteome

Leaf proteins extracted from leaf ranks 3 and 12 of ambient and high CO<sub>2</sub>-grown maize plants were separated using 2D gel electrophoresis (Supporting Information Table S4). Progenesis SameSpot 2D gel analysis software revealed the presence of about 900 spots in the leaf extracts. Relatively few spots were changed in abundance in rank 12 source leaves as a result of CO<sub>2</sub> enrichment. Growth with high CO<sub>2</sub> exerted the most pronounced effects on the proteome of rank 3 source leaves but the differences between differentially expressed proteins were generally less than twofold (Supporting Information Table S4). Sixty differentially-expressed spots were excised from the gels containing proteins of leaf rank 3 leaves and subjected to LCMS/MS analysis as outlined in the materials and methods section. In total, 69 proteins were identified from 35 protein spots (Supporting Information Table S4). Of these, 10 were increased in intensity and 25 spots were decreased in intensity in response to high CO<sub>2</sub> (Table 2). It is important to note that only 14 spot analyses resulted in the identification of a single protein, whereas the remaining 21 spots yielded between 2 and 7 different protein identifications per spot, making it difficult to determine precisely which protein was responsible for the increase or decrease in intensity of the respective spot. However, the FtSH protease was identified in three different spots (23, 24 and 34), all of which showed an approximately twofold decrease in response to high CO<sub>2</sub>. Many of the other identified proteins are involved in primary metabolism, particularly photosynthesis and respiration. The third largest functional group amongst the

**Table 1.** A comparison of leaf C and N contents (% of dry weight), leaf C/N ratios and leaf temperatures (*T*<sub>leaf</sub> in °C) in 3-week-old maize plants grown either under ambient CO<sub>2</sub> conditions or with CO<sub>2</sub> enrichment. Values represent mean ± SE; *n* = 4. Superscript letters are significantly different (*P* < 0.05)

	Ambient CO <sub>2</sub>	CO <sub>2</sub> enrichment
C (%)	41.72 ± 0.41 <sup>a</sup>	41.64 ± 0.05 <sup>a</sup>
N (%)	3.23 ± 0.09 <sup>a</sup>	3.06 ± 0.30 <sup>a</sup>
C/N	12.94 ± 0.23 <sup>a</sup>	13.72 ± 1.40 <sup>a</sup>
<i>T</i> <sub>leaf</sub> at 700 μL L <sup>-1</sup>	27.77 ± 0.41 <sup>b</sup>	28.80 ± 0.17 <sup>a</sup>
<i>T</i> <sub>leaf</sub> at 380 μL L <sup>-1</sup>	27.60 ± 0.36 <sup>b</sup>	28.63 ± 0.25 <sup>a</sup>

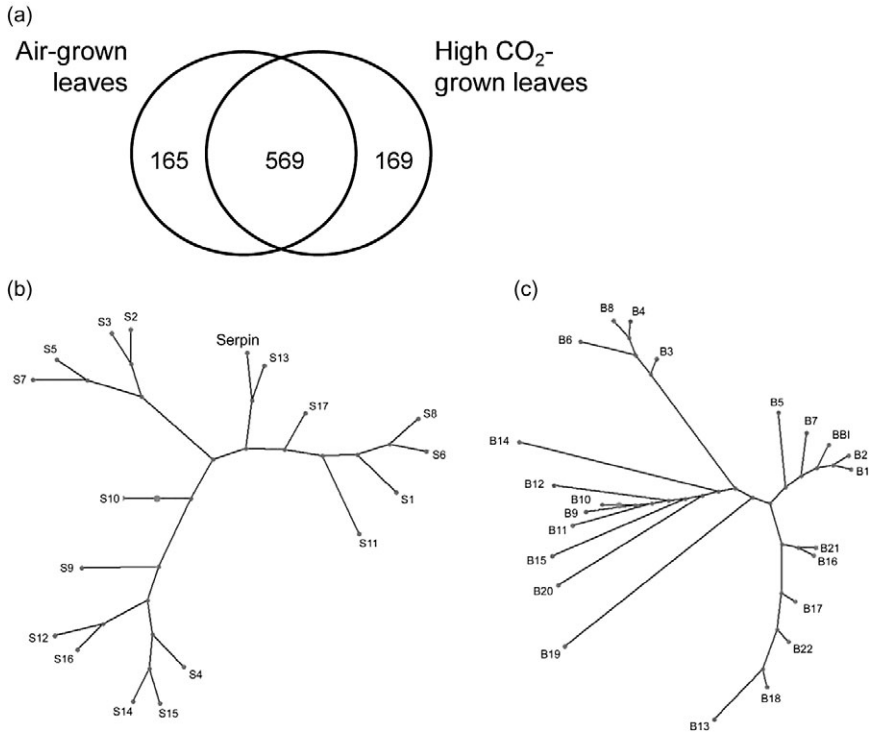


**Figure 3.** A comparison of transcripts responsive to leaf ontogeny under either ambient CO<sub>2</sub> conditions (Air-grown leaves) or with CO<sub>2</sub> enrichment (High CO<sub>2</sub>-grown leaves; a). Phylogenetic trees showing the relationships between putative serpin and known serine proteinase inhibitor protein sequences (S1–S17; b) and putative BBI and known Bowman–Birk serine protease inhibitor protein sequences (B1–B22, c) listed in Table 4.

proteins altered in response to high CO<sub>2</sub> were enzymes involved in protein metabolism (Table 2).

**Effects of sugars and cellular redox modulators on the abundance of maize leaf transcripts**

The data shown in Fig. 5a, b, indicated that the abundance of transcripts encoding the serpin and BBI inhibitors were

changed by the growth CO<sub>2</sub> level in a leaf rank specific manner. To determine whether the expression of serpin and BBI was influenced by sugars or subject to redox regulation, maize leaf pieces were incubated in solutions containing either sugars (sucrose, glucose or fructose) or pro-oxidants [hydrogen peroxide or methyl viologen (MV)]. Although the sugars had very little effect on the abundance of the transcripts associated with sugar

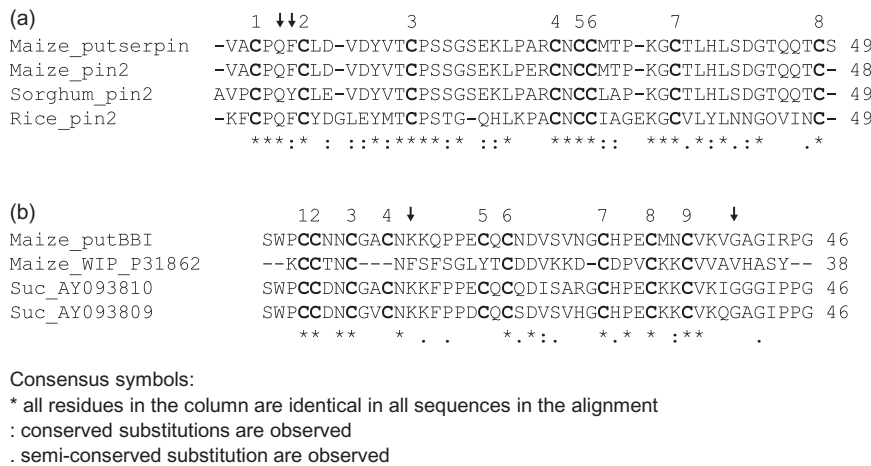


**Figure 4.** Multiple alignment of the identified serine proteinase inhibitor protein sequences with those of known serine proteinase inhibitors available in the database. Maize\_putserpin – putative maize serpin (EF406275). Maize\_pin2 (AI947362), Sorghum\_pin2 (AI724716), Rice\_pin2 (AU163886) – serine protease inhibitors identified in maize, sorghum, and rice, respectively. Maize\_putBBI – putative maize BBI (EF406276). Suc\_AY093810 and Suc\_AY093809 – two BBI sequences identified in *S. officinarum*. Maize\_WIP\_P31862 – a wound-induced protein from maize. Conserved cysteine residues that participate in disulphide bridges are numbered. Arrows indicate the putative protease-contact residues (Barta *et al.* 2002). Consensus symbols indicate: \* – all residues in the column are identical in all sequences in the alignment; : – conserved substitutions are observed; . – semi-conserved substitutions are observed.

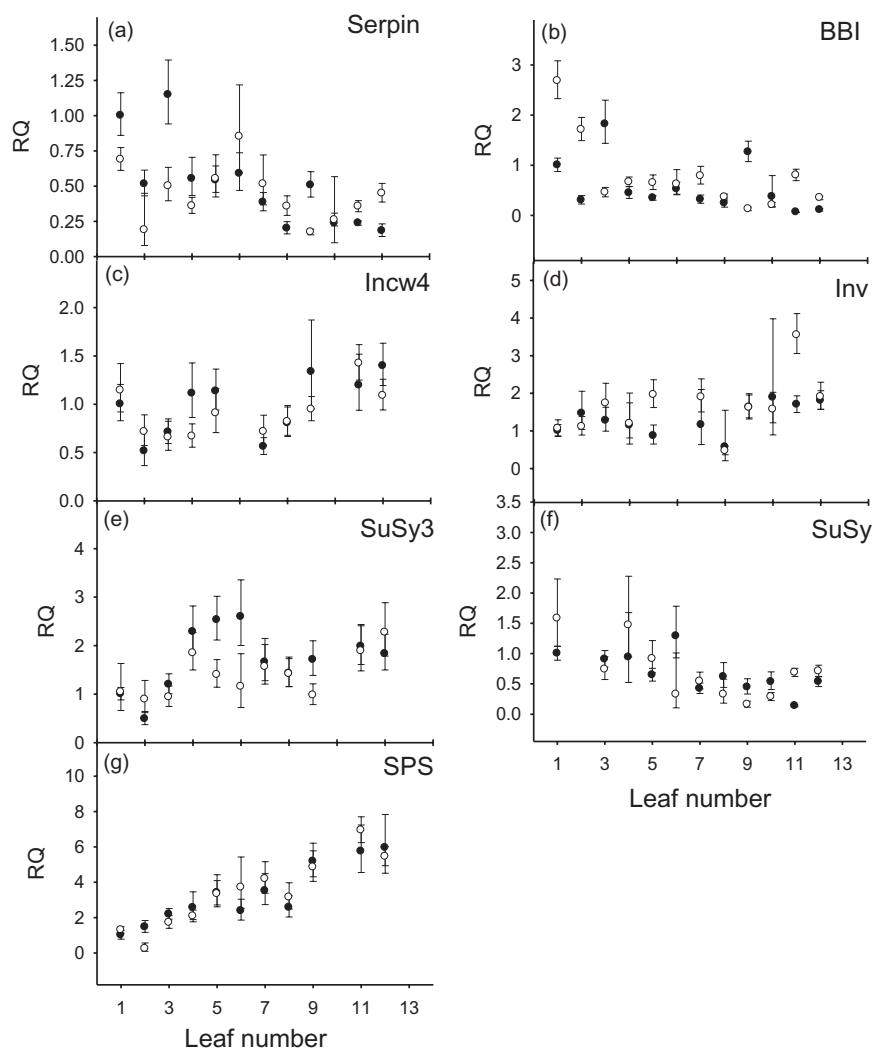


**Figure 5.** The effects of CO<sub>2</sub> enrichment on leaf rank-specific transcript levels measured by qPCR. Plants were grown for 8 weeks under either ambient CO<sub>2</sub> conditions (closed circles) or with CO<sub>2</sub> enrichment (open circles). The abundance of transcripts encoding serpin (a) BBI (b) cell wall invertase (c), invertase (d), sucrose synthase 3 (e), sucrose synthase (f), and sucrose phosphate synthase (g) was determined in all the leaves. Values  $\pm$  max/min are normalized to leaf 1 grown under ambient CO<sub>2</sub> conditions (RQ = 1) and expressed relative to endogenous controls.

metabolism, incubation with sucrose, fructose or glucose increased the abundance of serpin transcripts and decreased the levels of BBI transcripts (Table 3). Treatment with H<sub>2</sub>O<sub>2</sub> and methyl viologen increased the levels of both serpin and BBI transcripts but caused a small decrease the abundance of transcripts associated with sugar metabolism (Table 3).

### The effect of growth CO<sub>2</sub> levels on the leaf metabolome

Growth with high CO<sub>2</sub> had very little effect on maize leaf metabolite profiles (Supporting Information Table S5). Significant differences were found in only 13 metabolites in leaf rank 5 of 9-week-old plants. No significant changes in photorespiratory metabolites such as glycolate, glycerate, glycine or serine were found. The levels of leaf glucose, mannose and galactose were enhanced as a result of growth with CO<sub>2</sub> enrichment as were the levels of linoleic and linolenic acids (Fig. 6). Significant decreases were observed

only in glutarate, 2-hydroxyglutarate, 2-oxoglutarate, alanine, proline, myo-inositol and two isomers of hydroxybenzoate (Fig. 6).

### The effect of growth CO<sub>2</sub> levels on the leaf-rank-specific accumulation of carbohydrate and on associated enzymes

High CO<sub>2</sub> had a marked effect on the leaf rank-specific profile of carbohydrates but there was little effect on the activities of key enzymes involved in carbohydrate metabolism (Fig. 7). Glucose and fructose were much higher in the leaf ranks 1–5 compared with all other leaves on the stem, which had very low hexose contents when plants were grown under ambient CO<sub>2</sub> conditions (Fig. 7a, b). Growth with CO<sub>2</sub> enrichment completely suppressed this leaf rank-dependent change in leaf hexoses such that all the leaves had similar low amounts of glucose and fructose in this condition (Fig. 7a). Leaf sucrose (Fig. 7c) and starch (Fig. 7d) were not greatly changed as a result of leaf rank in plants grown under ambient CO<sub>2</sub> conditions. However,

**Table 2.** Proteins involved in protein metabolism that occur in 2DE spots of which the intensity is modulated by CO<sub>2</sub> enrichment at leaf rank 3 of plants grown for 8 weeks under either ambient CO<sub>2</sub> conditions (350 ± 20 µL L<sup>-1</sup>) or with CO<sub>2</sub> enrichment (700 ± 20 µL L<sup>-1</sup>)

Ratio CO <sub>2</sub> (High)/ CO <sub>2</sub> (Low)	Spot No	Migration first dim (cm)	Migration second dim (cm)	Identifier	Single protein ID in spot	Log(I)	rI	Log(e)	pI	Mr (kDa)	Description
1.95	27	5.1	7.8	LOC_Os08g03640.1		6.57	4	-4.6	5.4	34.4	60S acidic ribosomal protein P0 [ <i>Oryza sativa</i> (japonica cult
1.45	92	1.8	8.8	LOC_Os04g55650.1	✓	5.69	1	-7.8	5.7	28.4	Cysteine proteinase RD21a precursor, putative, expressed
-1.45	91	10.5	5.9	LOC_Os02g55420.1		5.51	1	-3.0	8.2	50.3	Aspartate aminotransferase, chloroplast precursor, putative, expressed
-1.46	89	7.8	7.5	LOC_Os08g03640.1		5.42	1	-3.9	5.4	34.4	60S acidic ribosomal protein P0 [ <i>Oryza sativa</i> (japonica cult
-1.46	87	9.6	4.9	LOC_Os01g36890.1		5.07	1	-3.0	5.5	48.6	Spliceosome RNA helicase BAT1, putative, expressed
-1.61	49	14	6.2	LOC_Os02g55420.1		5.40	1	-7.2	8.2	50.3	Aspartate aminotransferase, chloroplast precursor, putative, expressed
-1.67	48	7.3	5.4	LOC_Os02g05330.1		6.56	7	-55.7	5.4	47.1	Eukaryotic initiation factor 4A, putative, expressed
-1.67	48	7.3	5.4	LOC_Os01g71270.1		5.54	1	-4.4	5.3	49.0	Eukaryotic peptide chain release factor subunit 1-2, putative, expressed
-1.74	42	9.6	3.2	LOC_Os06g36700.1		5.67	2	-10.8	5.7	59.1	T-complex protein 1 subunit epsilon, putative, expressed
-1.81	34	6.4	3.2	LOC_Os06g45820.1	✓	6.79	14	-115.0	5.5	72.5	OsFtsH2 - <i>Oryza sativa</i> FtsH protease, homolog of AtFtsH2/8, expressed
-1.99	24	6.8	3.2	LOC_Os06g45820.1	✓	7.03	9	-64.0	5.5	72.5	OsFtsH2 - <i>Oryza sativa</i> FtsH protease, homolog of AtFtsH2/8, expressed
-2	23	7.1	3.2	LOC_Os06g45820.1		6.01	6	-55.3	5.5	72.5	OsFtsH2 - <i>Oryza sativa</i> FtsH protease, homolog of AtFtsH2/8, expressed
-2.29	16	10.5	2.3	LOC_Os01g01830.1		5.53	1	-6.1	5.3	82.0	Prolyl endopeptidase, putative, expressed

Column titles are: ratio CO<sub>2</sub>(high)/CO<sub>2</sub>(low); -fold change of spot intensities as measured from two-dimensional (2D) gel; Spot no: Spot number as numbered on 2D gel; migration first dim (cm): migration of the protein in the isoelectric focussing dimension on the 2D gel, migration second dim (cm): migration of the protein in the SDS-PAGE dimension on the 2D gel; Identifier: Database accession code of spot homolog; log(I): base 10 logarithm of the sum of the intensities of all the MS S spectra that contributed to the protein identification event; log(e): base 10 logarithm of the probability that a protein identification is a random event; pI: predicted isoelectric point of an identified protein; Mr: predicted molecular weight of an identified protein; Description: text-based description of an identified protein obtained from the database search or a BLAST-based homology search.

**Table 3.** Effects of sugars and pro-oxidants on the abundance of serpin and BBI transcripts and on selected transcripts encoding enzymes involved in sugar metabolism

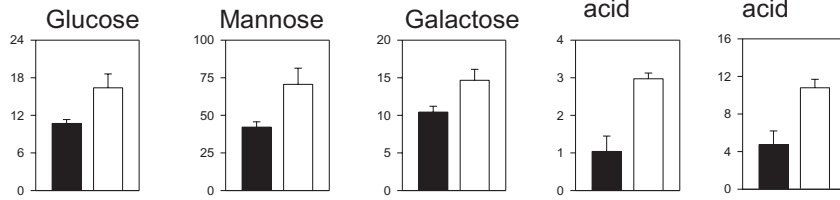
		Treatment				
		Sucrose	Fructose	Glucose	H <sub>2</sub> O <sub>2</sub>	MV
Transcript	Serpin	1.83 (1.64–2.04)	1.59 (1.19–2.12)	1.44 (1.34–1.54)	2.91 (2.51–3.38)	7.56 (6.05–9.47)
	BBI	0.54 (0.48–0.61)	0.52 (0.32–0.85)	0.44 (0.38–0.51)	1.97 (1.71–2.27)	1.32 (1.15–1.52)
	Incw4	0.96 (0.86–1.07)	0.95 (0.79–1.13)	0.72 (0.67–0.78)	0.78 (0.66–0.92)	0.91 (0.76–1.10)
	Inv	0.82 (0.54–1.24)	1.31 (0.96–1.80)	1.04 (0.89–1.21)	0.32 (0.24–0.42)	0.66 (0.56–0.78)
	SuSy3	1.12 (0.94–1.33)	1.29 (1.07–1.55)	1.17 (1.03–1.34)	0.45 (0.32–0.64)	1.70 (1.52–1.89)
	SuSy	1.22 (0.99–1.49)	1.07 (0.72–1.60)	0.72 (0.67–0.77)	1.81 (1.44–2.28)	0.78 (0.62–0.98)
	SS	0.91 (0.74–1.11)	1.18 (1.00–1.40)	0.76 (0.72–0.81)	0.30 (0.25–0.35)	0.77 (0.67–0.87)

Data represent relative minimum–maximum values calculated from at least three technical replicates normalized to values obtained from leaves incubated with buffer alone and relative to cyclophilin and ubiquitin as endogenous controls.

**Table 4.** Identified Bowman–Birk serine protease

	Sequence	Accession	Definition
<i>Serpin</i>	Serpin	EF406275.1	<i>Zea mays</i> putative serine type endopeptidase inhibitor
	S1	Q43502	Proteinase inhibitor type-2 CEVI57 precursor
	S2	AAF18450.1	Proteinase inhibitor type II precursor NGPI-1 [ <i>Nicotiana glutinosa</i> ]
	S3	AAF18451.1	Proteinase inhibitor type II precursor NGPI-2 [ <i>Nicotiana glutinosa</i> ]
	S4	ABA42892.1	Trypsin proteinase inhibitor precursor [ <i>Nicotiana benthamiana</i> ]
	S5	ABA42904.1	Trypsin proteinase inhibitor precursor [ <i>Nicotiana acuminata</i> ]
	S6	AAL54921.2	Proteinase inhibitor IIb [ <i>Solanum americanum</i> ]
	S7	AAR84197.1	Putative 6 repeat proteinase inhibitor [ <i>Nicotiana attenuata</i> ]
	S8	AAR37362.1	Proteinase inhibitor 2b precursor [ <i>Solanum nigrum</i> ]
	S9	AAQ56588.1	6-domain trypsin inhibitor precursor [ <i>Nicotiana attenuata</i> ]
	S10	AAO85558.1	7-domain trypsin inhibitor precursor [ <i>Nicotiana attenuata</i> ]
	S11	Q40561	Proteinase inhibitor type-2 precursor
	S12	ABA86556.1	Six domain proteinase inhibitor [ <i>Nicotiana tabacum</i> ]
	S13	BAA95792.1	Proteinase inhibitor II [ <i>Nicotiana tabacum</i> ]
	S14	AAZ20771.1	Insect injury-induced proteinase inhibitor [ <i>Nicotiana tabacum</i> ]
	S15	AAF14181.1	Proteinase inhibitor precursor [ <i>Nicotiana alata</i> ]
	S16	AAA17739.1	Proteinase inhibitor precursor
S17	P01080	Proteinase inhibitor type-2 K precursor	
<i>BBI</i>	BBI	EF406276.1	<i>Zea mays</i> putative Bowman–Birk serine protease inhibitor
	B1	ABL63911.1	Bowman–Birk serine proteinase inhibitor [ <i>Musa acuminata</i> ]
	B2	P81713	Bowman–Birk type trypsin inhibitor (WTI)
	B3	AAO89510.1	Bowman–Birk protease inhibitor [ <i>Glycine microphylla</i> ]
	B4	BAB86783.1	Bowman–Birk type proteinase iso-inhibitor A1 [ <i>Glycine soja</i> ]
	B5	P16343	Bowman–Birk type proteinase inhibitor DE-4 (DE4)
	B6	BAB86784.1	Bowman–Birk type proteinase iso-inhibitor A2 [ <i>Glycine soja</i> ]
	B7	P82469	Bowman–Birk type proteinase inhibitor 1
	B8	P01055	Bowman–Birk type proteinase inhibitor precursor (BBI)
	B9	P81484	Bowman–Birk type proteinase inhibitor PVI-3(2)
	B10	P81483	Bowman–Birk type proteinase inhibitor PVI-4
	B11	CAD32699.1	Double-headed trypsin inhibitor [ <i>Phaseolus vulgaris</i> ]
	B12	CAD32698.1	Double-headed trypsin inhibitor [ <i>Phaseolus vulgaris</i> ]
	B13	S09415	Proteinase inhibitor – cowpea
	B14	Q9S9E3	Horsegram inhibitor 1
	B15	CAL69237.1	Double-headed trypsin inhibitor [ <i>Phaseolus parvulus</i> ]
	B16	ABD91575.1	Trypsin inhibitor [ <i>Vigna radiata</i> var. <i>sublobata</i> ]
	B17	AAW84292.1	Trypsin inhibitor [ <i>Lens culinaris</i> ]
	B18	AAO43982.1	Trypsin inhibitor [ <i>Vigna unguiculata</i> subsp. <i>sesquipedalis</i> ]
	B19	P01059	Bowman–Birk type proteinase inhibitor DE-4
	B20	P01056	Bowman–Birk type proteinase inhibitor
	B21	ABD91574.1	Trypsin inhibitor [ <i>Vigna trilobata</i> ]
B22	CAC81081.1	Trypsin inhibitor [ <i>Vigna unguiculata</i> ]	

Increased at high CO<sub>2</sub>



Decreased at high CO<sub>2</sub>

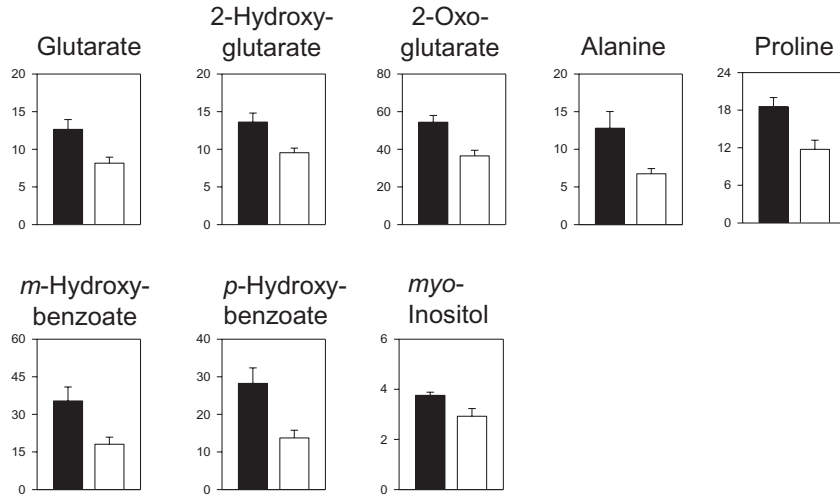


**Figure 6.** Effects of high CO<sub>2</sub> on maize leaf metabolite profiles. Plants were grown for 6 weeks under either ambient CO<sub>2</sub> conditions or with CO<sub>2</sub> enrichment. For a full data list, see Table S5. Note that peak intensities are in arbitrary units for each metabolite. Black bars, air. White bars, high CO<sub>2</sub>. Data are means ± SE (*n* = 4).

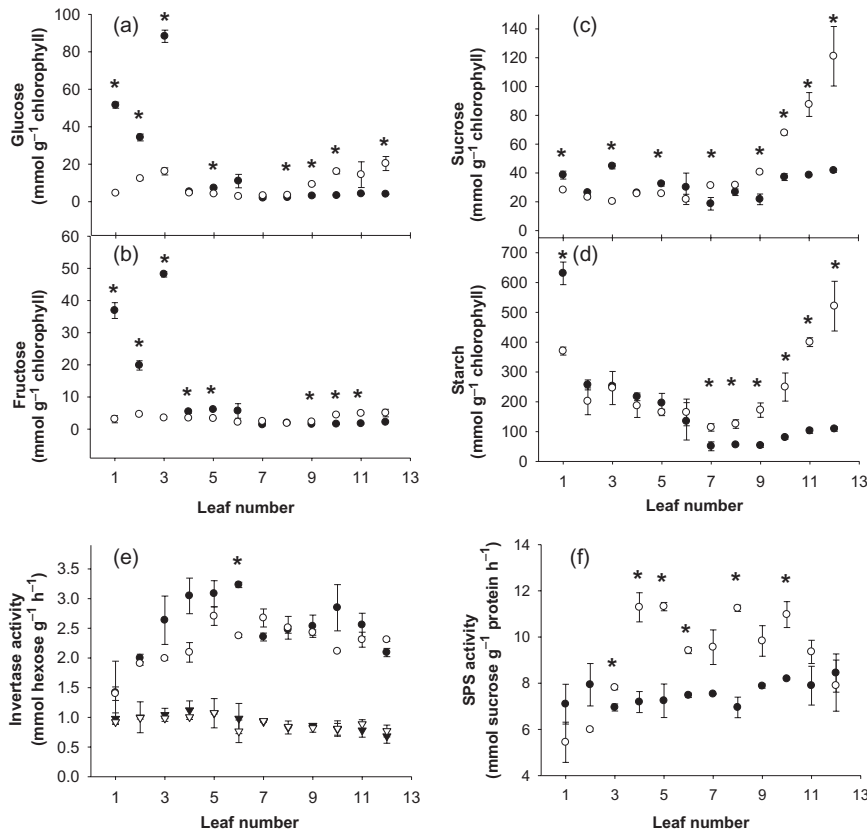


**Figure 7.** The effects of CO<sub>2</sub> enrichment on leaf rank-specific levels of hexoses, sucrose and starch and activities of sucrose phosphate synthase (SPS) and invertase. Plants were grown for 8 weeks under either ambient CO<sub>2</sub> conditions (closed circles) or with CO<sub>2</sub> enrichment (open circles). Glucose (a) fructose (b) sucrose (c) and starch (d) were determined in all the leaves as were the activities of sucrose phosphate synthase (e) in leaves under ambient CO<sub>2</sub> conditions (closed symbols) or with CO<sub>2</sub> enrichment (open symbols). Significant differences at *P* < 0.05 indicated by the symbol (\*).

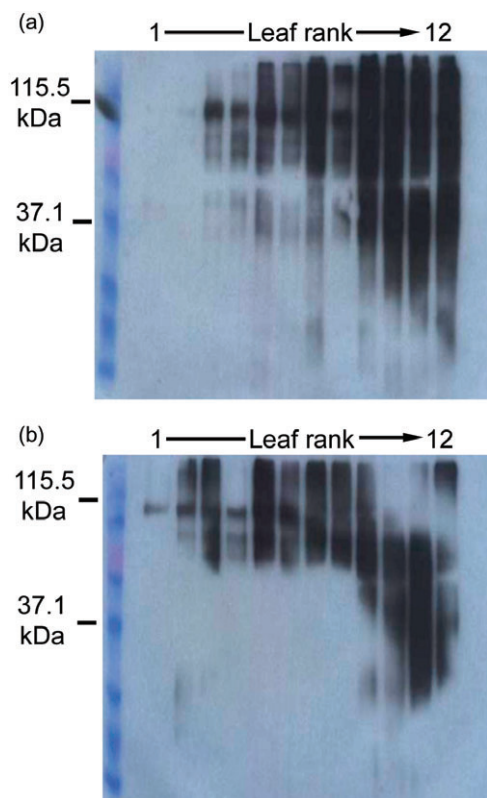


**Figure 8.** The effects of CO<sub>2</sub> enrichment on the leaf rank-specific abundance of protein carbonyl groups. Plants were grown for 8 weeks under either ambient CO<sub>2</sub> conditions (a) or with CO<sub>2</sub> enrichment (b). Protein carbonyl groups are compared for all leaves on the stem from leaf rank 1 to leaf rank 12.

there was a sharp increase in both of these carbohydrates in the leaf ranks 7–13 of plants grown with CO<sub>2</sub> enrichment.

Soluble acid invertase activities were much higher than those of neutral invertase in all but leaf ranks 10–13 of plants on the stem (Fig. 7e). Although neutral and acid invertase activities were unaffected by growth CO<sub>2</sub> level (Fig. 7e), SPS activities were markedly increased as a result of growth with CO<sub>2</sub> enrichment, in all but leaf ranks 1–3 and 10–13 (Fig. 7f).

### The effect of growth CO<sub>2</sub> level on the leaf-rank-specific accumulation of protein carbonyl groups

The extent of protein carbonyl group formation is controlled by leaf development in *Arabidopsis* (Johansson, Olsson & Nystrom 2004) but it is often used as a measure of cellular oxidation, as it increases in response to stress (Kingston-Smith & Foyer 2000). Leaf rank specific changes in the content of protein carbonyl group formation were apparent in maize (Fig. 8) like *Arabidopsis* leaves (Johansson *et al.* 2004). However, in the case of maize, protein carbonyls were most abundant in leaves 9–12 and they decreased progressively to leaf rank 1, which showed only

one detectable band of carbonyl groups in plants grown under ambient CO<sub>2</sub> conditions (Fig. 8a). The intensity of this single carbonyl-stained protein in leaf ranks 1 and 2 was increased in plants grown at high CO<sub>2</sub> (Fig. 8b). While growth with CO<sub>2</sub> enrichment had a dramatic effect on the profile of leaf carbonyl abundance and composition, the effect varied with leaf rank. The number of protein bands showing staining for protein carbonyl group was decreased in leaves 9–12 (Fig. 8b). In particular, there was a marked decrease in the number of high molecular weight proteins showing carbonyl group formation in leaves 9–12 at high CO<sub>2</sub> (Fig. 8). With exception of leaf ranks 1–4, the level of protein carbonyl formation was also modified in other leaf ranks but this effect was highly dependent on the molecular weight band analyzed (Fig. 8).

### DISCUSSION

While future increases in atmospheric CO<sub>2</sub> availability will benefit plants with the C<sub>3</sub> photosynthetic pathway, the nature of the responses of C<sub>4</sub> plants to elevated CO<sub>2</sub> remains controversial (Leakey 2009). Evidence from the Free-Air Concentration Enrichment Experiments (FACE) has consistently shown that growth with elevated CO<sub>2</sub> does not enhance maize leaf photosynthesis or plant growth (Leakey *et al.* 2006; 2009a,b). The results presented here confirm the observations from the FACE experiments and also data from other similar studies (Kim *et al.* 2006). Similarly, the leaf transcriptome analysis failed to show any significant differences between the air and high CO<sub>2</sub> samples in line with earlier observations (Kim *et al.* 2006; Leakey *et al.* 2009a, b). However, further analysis using qPCR revealed that transcripts encoding a BBI and a serpin were differentially expressed in relation to the growth CO<sub>2</sub> level in a leaf rank-specific manner. Similarly, the leaf proteome analysis suggested that several chloroplast proteins including components of the photosystem II (PSII) oxygen evolving complex and the ATP synthase were decreased at high CO<sub>2</sub> but only in the older source leaves. Of the proteins that were altered in abundance at high CO<sub>2</sub>, there was a marked effect on FtsH proteases, which are important in chloroplast biogenesis and thylakoid maintenance. The high CO<sub>2</sub>-dependent decreases in FtsH proteases may reflect the diminished requirement for photosystem repair in the older source leaves at high CO<sub>2</sub> compared with ambient CO<sub>2</sub>. These modest adjustments in chloroplast components were not however sufficient to cause a significant decrease in the overall rate of leaf photosynthesis. Analysis of the leaf metabolome showed that while metabolites associated with photorespiration were similar in leaves under ambient and high CO<sub>2</sub> conditions, the levels of some carbohydrates such as glucose, mannose and galactose were enhanced in the older source leaves as a result of growth with CO<sub>2</sub> enrichment. Similarly, spectrophotometric measurements of leaf starch, sucrose, glucose and fructose showed that these metabolites were modified as a result of growth with CO<sub>2</sub> enrichment. However, such changes in metabolite levels were dependent on the leaf position on the stem. Taken

together, the data suggest that maize leaves show acclimation to CO<sub>2</sub> enrichment. However, this trait occurs in a strict leaf-specific manner. Leaf ontogeny has a marked influence on leaf responses to atmospheric CO<sub>2</sub> availability. Maize leaves undergo a shift in photosynthesis from C<sub>3</sub> to C<sub>4</sub> metabolism during development (Crespo *et al.* 1979) and large number of transcripts were significantly changed in abundance between leaf ranks 3 and 12.

A key question that remains to be addressed concerns whether leaves are able to sense and signal changes in atmospheric CO<sub>2</sub> by pathways that are independent of photosynthesis. One mechanism that has been proposed implicates carbonic anhydrases in plant CO<sub>2</sub>-signalling pathways (Hu *et al.* 2010). While the data presented here do not provide any new insights into the roles of carbonic anhydrases in the CO<sub>2</sub>-signalling pathways in maize, the data clearly demonstrate that the acclimation responses to high CO<sub>2</sub> observed in maize are dependent on leaf rank. Thus, we explored how different parameters associated with leaf physiology were affected by growth at ambient and high CO<sub>2</sub>. The most pronounced effects were observed in the leaf transpiration rates, which were decreased in leaves grown at high CO<sub>2</sub> (Fig. 2). As a consequence of decreased transpiration rates, the leaf temperature were slightly increased in plants grown at high CO<sub>2</sub> (Table 1). However, the overall changes in maize leaf temperatures are very small, as observed previously (Kim *et al.* 2006). Thus, it is unlikely that CO<sub>2</sub>-dependent changes in leaf temperature are responsible for the observed changes in the leaf proteins, transcripts and metabolites. It has previously been suggested that high CO<sub>2</sub>-dependent changes in leaf metabolism are related to altered leaf N status (Kim *et al.* (2006). However, in the present experiments neither maize leaf N status nor leaf C/N ratios were significantly changed as a result of growth at high CO<sub>2</sub>.

Drought stress can be ameliorated at elevated CO<sub>2</sub> even in C<sub>4</sub> plants as a result of lower stomatal conductance and thus it is possible that maize leaves may be much less susceptible to water deficits when grown with CO<sub>2</sub> enrichment. Thus, the observed differences in transcripts, proteins and metabolites between the less photosynthetically-active leaves (ranks 3–5) and the younger (rank 12) source leaves may be related to slight changes in leaf water status. The stomatal conductance rates were significantly higher in leaves under ambient CO<sub>2</sub> conditions (Fig. 2b). While transpiration rates (Fig. 2a) and water use efficiency values (Fig. 2d) were similar in leaf rank 12 under both CO<sub>2</sub> conditions, the differences were significant in the older less photosynthetically active leaves (rank 5). The small CO<sub>2</sub>-dependent differences in the water status of the rank 12 leaves could therefore be responsible for the observed variations in transcripts, proteins and metabolites.

The decreased abundance of myo-inositol and two hydroxybenzoic acids, which are related to SA metabolism, were repressed at high CO<sub>2</sub> and there was a decreased abundance of protein carbonyl groups. These findings are consistent with a lower oxidative load in leaves grown

under high CO<sub>2</sub> conditions. This may be particularly important for bundle sheath proteins, which are more sensitive to carbonylation in response to cellular oxidation than those of the mesophyll (Kingston-Smith & Foyer 2000). The lower levels of protein oxidation under high CO<sub>2</sub> conditions are indicative of an altered cellular redox status, particularly in the younger leaf ranks. Alterations in cellular redox status may have important implications for enzymes and metabolic processes such as starch metabolism (Hendriks *et al.* 2003; Kolbe *et al.* 2005; Sparla *et al.* 2006) that are subject to redox regulation (Buchanan & Balmer 2005; Schürmann & Buchanan 2008).

Growth with high CO<sub>2</sub> exerted a marked influence on leaf carbohydrate status in a strict leaf-rank specific manner and this also might be related to changes in whole plant water status. A CO<sub>2</sub>-dependent accumulation of sucrose was observed only in the youngest leaves (ranks 9–12) but high CO<sub>2</sub> prevented the accumulation of hexoses in the older (ranks 1–3) leaves. These changes in the leaf carbohydrate profiles occurred in the absence of any detectable changes in the activities of key enzymes involved in carbohydrate metabolism but it might be related to decreased assimilate export from the younger leaves at high CO<sub>2</sub>. Interestingly, sugars are involved systemic signalling pathways that convey information concerning CO<sub>2</sub> availability from leaf to leaf (Coupe *et al.* 2006; Miyazawa *et al.* 2006; Baena-González *et al.* 2007). The failure of the older leaves to accumulate hexoses when grown under high CO<sub>2</sub> might also be related to decreased sucrose export from the younger leaves, particularly if this was associated with futile cycling between sucrose and hexoses (Nguyen-Quoc & Foyer 2001).

The functions of BBI and the serpin that were differentially expressed in relation to the growth CO<sub>2</sub> level in a leaf rank-specific manner are not known. The serpin (EF406275) is homologous to an *Arabidopsis* serine-type endopeptidase inhibitor (AT1G72060) and has signal peptide and pin2 domains. The BBI protein has a theoretical molecular weight of 10.4 kDa and pI of 6.01 with signal peptide and BB leg domains. The signal peptides suggest that both proteins are targeted to classical secretory pathways and therefore may be involved in autophagocytotic pathways of protein degradation associated with the vesicular transport system or with processes located in the extracellular/apoplastic space. The vesicular trafficking system has functions linked to plant stress responses (Leshem *et al.* 2006) and to the degradation of Rubisco and other chloroplast proteins (Chiba *et al.* 2003; Ishida *et al.* 2007; Prins *et al.* 2008).

While plant serpins have been intensively studied particularly in cereal seeds, relatively few protein targets have been identified to date and precise roles have yet to be assigned. One target has been shown to be the cysteine-dependent protease, metacaspase 9, which is strongly inhibited by *Arabidopsis* Serpin1. However, the *in vitro* inhibition of trypsin and metacaspase 4 imply that Serpin1 has a range of targets (Vercammen *et al.* 2006).

The serpin and BBI transcripts were most abundant in the older leaf ranks 1–3, which is consistent with roles in

autophagocytotic pathways of protein degradation. Their expression patterns of these protease inhibitors were changed by growth at high CO<sub>2</sub> in the older source leaves and further examination revealed that the abundance of the transcripts was modulated in response to sugars and redox effectors. The serpin transcripts were increased in the presence of sugars while the BBI transcripts were repressed under these conditions. The abundance of serpin transcripts was lower in the older source leaves grown at high CO<sub>2</sub>, consistent with the high CO<sub>2</sub>-dependent decrease in leaf hexoses. These results may implicate sugar signalling in the regulation of serpin expression at high CO<sub>2</sub>. However, CO<sub>2</sub>-dependent alterations in sugar signalling do not appear to be involved in the regulation of the expression of the BBI inhibitor.

## ACKNOWLEDGMENTS

This work was funded by a Royal Society (UK)-National Research Foundation (South Africa) joint project (GUN 2068793). A.P. thanks the Association of Commonwealth Universities for a split-site PhD fellowship between the labs of C.F. (UK) and K.K. (South Africa). M.S.S.L. thanks Fundacao para a Ciencia e a Tecnologia, Portugal for a fellowship (SFRH/BPD/34310/2006) to the Foyer lab. P.K. thanks the The Scottish Crop Research Institute, UK and the University of Leeds, UK for split site PhD fellowship. NEPAF is funded by ONE NorthEast (UK) and the European Regional Development Fund. Rothamsted Research receives grant-aided support from the UK Biotechnology and Biological Sciences Research Council.

## REFERENCES

- Acharya B.R. & Assmann S.M. (2009) Hormone interactions in stomatal function. *Plant Molecular Biology* **69**, 451–462.
- Altschul S.F., Gish W., Miller W., Myers E.W. & Lipman D.J. (1990) Basic local alignment search tool. *Journal of Molecular Biology* **215**, 403–410.
- Baena-González E., Rolland F., Thevelein J.M. & Sheen J. (2007) A central integrator of transcription networks in plant stress and energy signaling. *Nature* **448**, 938–943.
- Baroli I., Price G.D., Badger M.R. & Von Caemmerer S. (2008) The contribution of photosynthesis to the red light response of stomatal conductance. *Plant Physiology* **146**, 737–747.
- Barta E., Pintar A. & Pongor S. (2002) Repeats with variations: accelerated evolution of the Pin2 family of proteinase inhibitors. *Trends in Genetics* **18**, 600–603.
- Bradford M.M. (1976) A rapid and sensitive method for the quantitation of microgram quantities of protein utilizing the principle of protein-dye binding. *Analytical Biochemistry* **72**, 248–254.
- Buchanan B.B. & Balmer Y. (2005) Redox regulation: a broadening horizon. *Annual Review of Plant Biology* **56**, 187–220.
- Chiba A., Ishida H., Nishizawa N.K., Makino A. & Mae T. (2003) Exclusion of ribulose-15-bisphosphate carboxylase/oxygenase from chloroplasts by specific bodies in naturally senescing leaves of wheat. *Plant & Cell Physiology* **44**, 914–921.
- Coupe S.A., Palmer B.G., Lake J.A., Overy S.A., Oxborough K., Woodward F.I., Gray J.E. & Quick W.P. (2006) Systemic signalling of environmental cues in *Arabidopsis* leaves. *Journal of Experimental Botany* **57**, 329–341.
- Cousins A.B., Adam N.R., Wall G.W., et al. (2001) Reduced photorespiration and increased energy-use efficiency in young CO<sub>2</sub>-enriched sorghum leaves. *New Phytologist* **150**, 275–284.
- Craig R. & Beavis R.C. (2004) TANDEM: matching proteins with tandem mass spectra. *Bioinformatics* **20**, 1466–1467.
- Crespo H.M., Freaux M., Cresswell C.R. & Tew J. (1979) The occurrence of both C<sub>3</sub> and C<sub>4</sub> photosynthetic characteristics in a single *Zea mays* plant. *Planta* **147**, 257–263.
- Croxdale J. (1998) Stomatal patterning in monocotyledons: *tridactantia* as a model system. *Journal of Experimental Botany* **49**, 279–292.
- Driscoll S.P., Prins A., Olmos E., Kunert K.J. & Foyer C.H. (2006) Specification of adaxial and abaxial stomata epidermal structure and photosynthesis to CO<sub>2</sub> enrichment in maize leaves. *Journal of Experimental Botany* **57**, 381–390.
- Emanuelsson O., Nielsen H., Brunak R. & Von Heijne G. (2000) Predicting subcellular localization of proteins based on their N-terminal amino acid sequence. *Journal of Molecular Biology* **300**, 1005–1016.
- Ferris R., Long L., Bunn S.M., Robinson K.M., Bradshaw H.D., Rae A.M. & Taylor G. (2002) Leaf stomatal and epidermal cell development: identification of putative quantitative trait loci in relation to elevated carbon dioxide concentration in poplar. *Tree Physiology* **22**, 633–640.
- Foyer C.H., Bloom A., Queval G. & Noctor G. (2009) Photorespiratory metabolism: genes, mutants, energetics, and redox signaling. *Annual Review of Plant Biology* **60**, 455–484.
- Fryer M.J., Ball L., Oxborough K., Karpinski S., Mullineaux P.M. & Baker N.R. (2003) Control of *Ascorbate Peroxidase 2* expression by hydrogen peroxide and leaf water status during excess light stress reveals a functional organisation of *Arabidopsis* leaves. *The Plant Journal* **33**, 691–705.
- Ghannoum O., Von Caemmerer S., Barlow E.W.R. & Conroy J.P. (1997) The effect of CO<sub>2</sub> enrichment and irradiance on the growth, morphology and gas-exchange of a C<sub>3</sub> (*Panicum laxum*) and a C<sub>4</sub> (*Panicum antidotale*) grass. *Australian Journal of Plant Physiology* **24**, 227–237.
- Ghannoum O., Von Caemmerer S. & Conroy J.P. (2001) Plant water use efficiency of 17 Australian NAD-ME and NADP-ME C<sub>4</sub> grasses at ambient and elevated CO<sub>2</sub> partial pressure. *Australian Journal of Plant Physiology* **28**, 1207–1217.
- Gish W. & States D.J. (1993) Identification of protein coding regions by database similarity search. *Nature Genetics* **3**, 266–272.
- Gray J.E., Holroyd G.H., Van Der Lee F.M., Bahrami A.R., Sijmons P.C., Woodward F.I., Schuch W. & Hetherington A.M. (2000) The HIC signalling pathway links CO<sub>2</sub> perception to stomatal development. *Nature* **408**, 713–716.
- Hendriks J.H.M., Kolbe A., Gibon Y., Stitt M. & Geigenberger P. (2003) ADP-glucose pyrophosphorylase is activated by post-translational redox-modification in response to light and to sugars in leaves of *Arabidopsis* and other plant species. *Plant Physiology* **133**, 838–849.
- Hu H., Boisson-Dernier A., Israelsson-Nordström M., Böhmer M., Xue S., Ries A., Godoski J., Kuhn J.M. & Schroeder J.I. (2010) Carbonic anhydrases are upstream regulators of CO<sub>2</sub>-controlled stomatal movements in guard cells. *Nature Cell Biol* **12**, 87–93.
- Ishida H., Yoshimoto K., Reisen D., Makino A., Ohsumi Y., Hanson M. & Mae T. (2007) Visualization of Rubisco-containing bodies derived from chloroplasts in living cells of *Arabidopsis*. *Photosynthesis Research* **91**, 275–276.
- Johansson E., Olsson O. & Nystrom T. (2004) Progression and specificity of protein oxidation in the life cycle of *Arabidopsis thaliana*. *Journal of Biological Chemistry* **279**, 22204–22208.

- Jones M.G.K., Outlaw J.W.H. & Lowry O.H. (1977) Enzymic assay of  $10^{-7}$  to  $10^{-14}$  moles of sucrose in plant tissues. *Plant Physiology* **60**, 379–383.
- Karpinski S., Reynolds H., Karpinska B., Wingsle G., Creissen G. & Mullineaux P. (1999) Systemic signaling and acclimation in response to excess excitation energy in *Arabidopsis*. *Science* **284**, 654–657.
- Khatiwala S., Primeau F. & Hall T. (2009) Reconstruction of the history of anthropogenic CO<sub>2</sub> concentrations in the ocean. *Nature* **462**, 346–349.
- Kim S.-H., Sicher R.C., Bae H., Gitz D.C., Baker J.T., Timlin D.J. & Reddy V.R. (2006) Canopy photosynthesis evapotranspiration leaf nitrogen and transcription profiles of maize in response to CO<sub>2</sub> enrichment. *Global Change Biology* **12**, 588–600.
- Kingston-Smith A.H. & Foyer C.H. (2000) Bundle sheath proteins are more sensitive to oxidative damage than those of the mesophyll in maize leaves exposed to paraquat or low temperatures. *Journal of Experimental Botany* **51**, 123–130.
- Kolbe A., Tiessen A., Schluepmann H., Paul M., Ulrich S. & Geigenberger P. (2005) Trehalose 6-phosphate regulates starch synthesis via posttranslational redox activation of ADP-glucose pyrophosphorylase. *Proceedings of the National Academy of Sciences of the United States America* **102**, 11118–11123.
- Lake J.A., Quick W.P., Beerling D.J. & Woodward F.I. (2001) Plant development: signals from mature to new leaves. *Nature* **411**, 154–158.
- Lake J.A., Woodward F.I. & Quick W.P. (2002) Long distance CO<sub>2</sub> signalling in plants. *Journal of Experimental Botany* **53**, 183–193.
- Larkin J.C., Marks M.D., Nadeau J. & Sack F. (1997) Epidermal cell fate and patterning in leaves. *The Plant Cell* **9**, 1109–1120.
- Leakey A.D.B. (2009) Rising atmospheric carbon dioxide concentration and the future of C4 crops for food and fuel. *Proceedings of the Royal Society B. Biological Sciences* **276**, 2333–2343.
- Leakey A.D.B., Uribelarrea M., Ainsworth E.A., Naidu S.L., Rogers A., Ort D.R. & Long S.P. (2006) Photosynthesis productivity and yield of maize are not affected by open-air elevation of CO<sub>2</sub> concentration in the absence of drought. *Plant Physiology* **140**, 779–790.
- Leakey A.D.B., Ainsworth E.A., Bernard S.M., et al. (2009a) Gene expression profiling – opening the black box of plant ecosystem responses to global change. *Global Change Biology* **15**, 1201–1213.
- Leakey A.D.B., Ainsworth E.A., Bernacchi C.J., Rogers A., Long S.P. & Ort D.R. (2009b) Elevated CO<sub>2</sub> effects on plant carbon, nitrogen and water relations: six important lessons from FACE. *Journal of Experimental Botany* **60**, 2859–2876.
- Leshem Y., Melamed-Book N., Cagnac O., Ronen G., Nishri Y., Solomon M., Cohen G. & Levine A. (2006) Suppression of *Arabidopsis* vesicle-SNARE expression inhibited fusion of H<sub>2</sub>O<sub>2</sub>-containing vesicles with tonoplast and increased salt tolerance. *Proceedings of the National Academy of Sciences of United States America* **103**, 18008–18013.
- Long S.P., Ainsworth E.A., Alistair R. & Ort D.R. (2004) Rising atmospheric carbon dioxide: plants FACE the future. *Annual Review of Plant Biology* **55**, 591–628.
- Long S.P., Zhu X.-G., Naidu S.L. & Ort D.R. (2006) Can improvement in photosynthesis increase crop yields? *Plant, Cell & Environment* **29**, 315–330.
- Maroco J.P., Edwards G.E. & Ku M.S.B. (1999) Photosynthetic acclimation of maize to growth under elevated levels of carbon dioxide. *Planta* **210**, 115–125.
- Martin C. & Glover B.J. (2007) Functional aspects of cell patterning in aerial epidermis. *Current Opinion in Plant Biology* **10**, 70–82.
- Masle J. (2000) The effects of elevated CO<sub>2</sub> concentrations on cell division rates, growth patterns, and blade anatomy in young wheat plants are modulated by factors related to leaf position, vernalization, and genotype. *Plant Physiology* **122**, 1399–1415.
- Miyazawa S.I., Livingston N.J. & Turpin D.H. (2006) Stomatal development in new leaves is related to the stomatal conductance of mature leaves in poplar (*Populus trichocarpa* x *P. deltoides*). *Journal of Experimental Botany* **57**, 373–380.
- Mott K.A. (1988) Do stomata respond to CO<sub>2</sub> concentrations other than intercellular? *Plant Physiology* **86**, 200–203.
- Mott K.A., Sibbersen E.D. & Shope J.C. (2008) The role of the mesophyll in stomatal responses to light and CO<sub>2</sub>. *Plant, Cell & Environment* **31**, 1299–1306.
- Muhlenbock P., Szechynska-Hebda M., Plaszczyca M., Baudo M., Mullineaux P.M., Parker J.E., Karpinska B. & Karpinski S. (2008) Chloroplast signalling and LESION SIMULATING DISEASE1 regulate crosstalk between light acclimation and immunity in *Arabidopsis*. *The Plant Cell* **20**, 2339–2356.
- Nguyen-Quoc B. & Foyer C.H. (2001) Sucrose metabolism in tomato fruit: 'Futile cycles' and distinct roles for invertase and sucrose synthase. *Journal of Experimental Botany* **52**, 881–889.
- Noctor G., Bergot G., Thominet D., Mauve C., Lelarge-Trouverie C. & Prioul J.L. (2007) A comparative study of amino acid analysis in leaf extracts by gas chromatography-time of flight-mass spectrometry and high performance liquid chromatography with fluorescence detection. *Metabolomics* **3**, 161–174.
- Paul M.J. & Foyer C.H. (2001) Sink regulation of photosynthesis. *Journal of Experimental Botany* **52**, 1383–1400.
- Paul M. & Stitt M. (1993) Effects of nitrogen and phosphate deficiencies on levels of carbohydrates respiratory enzymes and metabolites in seedlings of tobacco and their response to exogenous sucrose. *Plant, Cell & Environment* **16**, 1047–1057.
- Pontius J.U., Wagner L. & Schuler G.D. (2003) UniGene: a unified view of the transcriptome. In *The NCBI Handbook* National Center for Biotechnology Information, Bethesda (MD), p. 11.
- Poorter H. & Navas M.-L. (2003) Plant growth and competition at elevated CO<sub>2</sub>: on winners, losers and functional groups. *New Phytologist* **157**, 175–198.
- Prins A., Van Heerden P.D.R., Olmos E., Kunert K.J. & Foyer C.H. (2008) Cysteine proteinases regulate chloroplast protein content and composition in tobacco leaves: a model for dynamic interactions with ribulose-1 5-bisphosphate carboxylase/oxygenase (RuBisCO) vesicular bodies. *Journal of Experimental Botany* **50**, 1935–1950.
- Ramagli L.S. (1999) Quantifying protein in 2-D PAGE solubilization buffers. In *Methods in Molecular Biology* (ed. A.J. Link) **112**, pp. 99–103. Humana Press Inc, Totowa, NJ.
- Rossel J.B., Wilson P.B., Hussain D., Woo N.S., Gordon M.J., Mewett O.P., Howell K.A., Whelan J., Kazan K. & Pogson B.J. (2007) Systemic and intracellular responses to photooxidative stress in *Arabidopsis*. *The Plant Cell* **19**, 4091–4110.
- Sage R.F. (1994) Acclimation of photosynthesis to increasing atmospheric CO<sub>2</sub>: the gas exchange perspective. *Photosynthesis Research* **39**, 351–368.
- Schürmann P. & Buchanan B. (2008) The ferredoxin-thioredoxin system of oxygenic photosynthesis. *Antioxidants & Redox Signaling* **10**, 1235–1273.
- Sims D.A. & Gamon J.A. (2002) Relationships between leaf pigment content and spectral reflectance across a wide range of species leaf structures and developmental stages. *Remote Sensing of Environment* **81**, 337–354.
- Soares A.S., Driscoll S.P., Olmos E., Harbinson J., Arrabaça M.C. & Foyer C.H. (2007) Adaxial/abaxial specification in the regulation of photosynthesis with respect to light orientation and growth

- with CO<sub>2</sub> enrichment in the C<sub>4</sub> species *Paspalum dilatatum*. *New Phytologist* **177**, 186–198.
- Soares-Cordeiro A.S., Driscoll S.P., Pellny T.K., Olmos E., Arrabaca M.C. & Foyer C.H. (2009) Variations in the dorso-ventral organization of leaf structure and Kranz anatomy coordinate the control of photosynthesis and associated signalling at the whole leaf level in monocotyledonous species. *Plant, Cell & Environment* **32**, 1833–1844.
- Sparla F., Costa A., Lo Schiavo F., Pupillo R. & Trost P. (2006) Redox regulation of a novel plastid-targeted beta-amylase of *Arabidopsis*. *Plant Physiology* **141**, 840–850.
- Taylor G., Ranasinghe S., Bosac C., Gardner S.D.L. & Ferris R. (1994) Elevated CO<sub>2</sub> and plant growth: cellular mechanisms and responses of whole plants. *Journal of Experimental Botany* **45**, 1761–1774.
- Taylor G., Tallis M.J., Giardina C.P., et al. (2008) Future atmospheric CO<sub>2</sub> leads to delayed autumnal senescence. *Global Change Biology* **14**, 264–275.
- Vercammen D., Belenghi B., van de Cotte B., Beunens T., Gavigan J.-A., De Rycke R., Brackener A., Inzé D., Harris J.L. & Van Breusegem F. (2006) Serpin1 of *Arabidopsis thaliana* is a suicide inhibitor for metacaspase 9. *Journal of Molecular Biology* **364**, 625–636.
- Vernon L.P. (1960) Spectrophotometer determination of chlorophylls and pheophytins in plant extracts. *Analytical Chemistry* **32**, 1144–1150.
- von Caemmerer S., Lawson T., Oxborough K., Baker N.R., Andrews T.J. & Raines C.A. (2004) Stomatal conductance does not correlate with photosynthetic capacity in transgenic tobacco with reduced amounts of Rubisco. *Journal of Experimental Botany* **55**, 1157–1166.
- Wand S.J.E., Midgley G.F., Jones M.H. & Curtis P.S. (1999) Responses of wild C<sub>4</sub> and C<sub>3</sub> grass (*Poaceae*) species to elevated atmospheric CO<sub>2</sub> concentration: a meta-analytic test of current theories and perceptions. *Global Change Biology* **5**, 723–741.
- Wand S.J.E., Midgley G.F. & Stock W.D. (2001) Growth responses to elevated CO<sub>2</sub> in NADP-ME, NAD-ME and PCK C<sub>4</sub> grasses and a C<sub>3</sub> grass from South Africa. *Australian Journal of Plant Physiology* **28**, 13–25.
- Ward J.K., Tissue D.T., Thomas R.B. & Strain B.R. (1999) Comparative responses of model C<sub>3</sub> and C<sub>4</sub> plants to drought in low and elevated CO<sub>2</sub>. *Global Change Biology* **5**, 857–867.
- Warren C.R. (2008) Stand aside stomata, another actor deserves centre stage: the forgotten role of the internal conductance to CO<sub>2</sub> transfer. *Journal of Experimental Botany* **59**, 1475–1487.
- Wintermans J.F.G. & De Mots A. (1965) Spectrophotometric characteristics of chlorophyll *a* and *b* and their pheophytins in ethanol. *Biochimica et Biophysica Acta* **109**, 448–453.
- Woodward F.I. (2002) Potential impacts of global elevated CO<sub>2</sub> concentrations on plants. *Current Opinion in Plant Biology* **5**, 207–211.
- Woodward F.I. & Kelly C.K. (1995) The effect of CO<sub>2</sub> concentration on stomatal density. *New Phytologist* **131**, 311–327.
- Woodward F.I.J., Lake A. & Quick W.P. (2002) Stomatal development and CO<sub>2</sub>: ecological consequences. *New Phytologist* **153**, 477–484.
- Zhu J., Goldstein G. & Bartholomew D.P. (1999) Gas exchange and carbon isotope composition of *Ananas comosus* in response to elevated CO<sub>2</sub> and temperature. *Plant, Cell & Environment* **22**, 999–1007.
- Ziska L.H. & Bunce J.A. (1999) Effect of elevated carbon dioxide concentration at night on the growth and gas exchange of selected C<sub>4</sub> species. *Australian Journal of Plant Physiology* **26**, 71–77.

Received 16 May 2010; received in revised form 11 August 2010; accepted for publication 6 October 2010

## SUPPORTING INFORMATION

Additional Supporting Information may be found in the online version of this article:

**Table S1.** Transcripts differentially expressed in the 3rd leaf relative to the 12th leaf in air.

**Table S2.** Transcripts differentially expressed in the 3rd leaf relative to the 12th leaf in high CO<sub>2</sub>.

**Table S3.** Functional analysis of transcripts differentially expressed due to leaf rank regardless of growth CO<sub>2</sub>.

**Table S4.** Functional analysis of proteins differentially expressed due to CO<sub>2</sub> enrichment in old source leaves (leaf rank 3) of 8 week-old maize plants.

**Table S5.** Full list of metabolites detected in maize leaves by GC-TOF-MS and their respective abundances in air and at high CO<sub>2</sub>. Metabolites showing significant differences at  $P < 0.05$  are highlighted and their mean peak intensities in the two conditions are plotted as histograms in Fig. 6. Peak intensities are in arbitrary units for each metabolite.

Please note: Wiley-Blackwell are not responsible for the content or functionality of any supporting materials supplied by the authors. Any queries (other than missing material) should be directed to the corresponding author for the article.